


Fall 2004

Layer-by-layer self-assembly for enzyme and DNA encapsulation and delivery

Amish Patel
Louisiana Tech University

Follow this and additional works at: <https://digitalcommons.latech.edu/dissertations>

 Part of the [Biochemistry Commons](#), [Materials Science and Engineering Commons](#), and the [Pharmacology Commons](#)

Recommended Citation

Patel, Amish, "" (2004). *Dissertation*. 605.
<https://digitalcommons.latech.edu/dissertations/605>

This Dissertation is brought to you for free and open access by the Graduate School at Louisiana Tech Digital Commons. It has been accepted for inclusion in Doctoral Dissertations by an authorized administrator of Louisiana Tech Digital Commons. For more information, please contact digitalcommons@latech.edu.

NOTE TO USERS

This reproduction is the best copy available.

UMI[®]

**LAYER-BY-LAYER SELF-ASSEMBLY FOR ENZYME & DNA
ENCAPSULATION AND DELIVERY**

By

Amish Patel, M.S.

A Dissertation Presented in Partial Fulfillment
of the Requirements for the Degree
Doctor of Philosophy

COLLEGE OF ENGINEERING AND SCIENCE
LOUISIANA TECH UNIVERSITY

November 2004

UMI Number: 3148958

INFORMATION TO USERS

The quality of this reproduction is dependent upon the quality of the copy submitted. Broken or indistinct print, colored or poor quality illustrations and photographs, print bleed-through, substandard margins, and improper alignment can adversely affect reproduction.

In the unlikely event that the author did not send a complete manuscript and there are missing pages, these will be noted. Also, if unauthorized copyright material had to be removed, a note will indicate the deletion.

UMI[®]

UMI Microform 3148958

Copyright 2005 by ProQuest Information and Learning Company.

All rights reserved. This microform edition is protected against unauthorized copying under Title 17, United States Code.

ProQuest Information and Learning Company
300 North Zeeb Road
P.O. Box 1346
Ann Arbor, MI 48106-1346

LOUISIANA TECH UNIVERSITY

THE GRADUATE SCHOOL

11/04/2004
Date

We hereby recommend that the Dissertation prepared under our supervision by Amish Patel entitled "Layer-by-Layer Self-Assembly for Enzyme & DNA Encapsulation and Delivery" An Approach towards potential applications of drug delivery and sensors" be accepted in partial fulfillment of the requirements for the Degree of Doctor of Philosophy

Yusi Luou
Supervisor of Dissertation Research
[Signature]
Head of Department
Chemical Engr.
Department

Recommendation concurred in:

Yusi Luou
[Signature]
[Signature]
[Signature]
[Signature]

Advisory Committee

Approved:
[Signature]
Director of Graduate Studies

Approved:
[Signature]
Dean of the Graduate School

[Signature]
Dean of the College

ABSTRACT

Thin wall microcapsules were formed via Layer-by-Layer Self-Assembly of alternate adsorption of oppositely charged polyelectrolyte on microcores. After the core dissolution, empty polymeric shells with 20-25 nm thick walls were obtained. These microcapsules were loaded with Myoglobin, Hemoglobin and Glucose Oxidase by opening capsule pores at low pH and closing them at higher pH. The native structure of the enzyme was not affected due to different treatments. Biocompatible nanoshells were also prepared for encasing DNA. Using the same Layer-by-Layer Self-Assembly approach nanoparticle were constructed containing DNA as one of the layers. The nanoparticles of different architecture were used to deliver DNA to specific cell lines.

APPROVAL FOR SCHOLARLY DISSEMINATION

The author grants to the Prescott Memorial Library of Louisiana Tech University the right to reproduce, by appropriate methods, upon request, any or all portions of this Dissertation. It is understood that "proper request" consists of the agreement, on the part of the requesting party, that said reproduction is for his personal use and that subsequent reproduction will not occur without written approval of the author of this Dissertation. Further, any portions of the Dissertation used in books, papers, and other works must be appropriately referenced to this Dissertation.

Finally, the author of this Dissertation reserves the right to publish freely, in the literature, at any time, any or all portions of this Dissertation.



Author



Date

TABLE OF CONTENTS

List of Tables	vii
List of Figures	viii
Acknowledgments	x
1.Introduction	
1.1 Nanotechnology: Nano-organized Thin Film.....	1
1.2 Layer-by-Layer Self-Assembly Technique.....	4
1.2.1 L-b-L Self-Assembly as Applied to Flat Surfaces.....	5
1.2.2 L-b-L Self-Assembly as Applied to Colloids.....	7
1.3 Basics of Thin Film Adsorption.....	8
1.3.1 Protein Films	11
1.4 Formation of Capsules	13
1.4.1 Encapsulation	15
1.5 Ideology	18
1.5.1 Protein Loading.....	18
1.5.2 Nanoparticles for DNA Delivery Using LbL Technique.....	18
1.5.3 DNA Encasing	19
2.Materials and Methods	
2.1 Materials	20
2.1.1 Protein Loading Experiments.....	21
2.1.2 Nanoparticles for DNA Delivery Experiments.....	22
2.1.3 DNA Encasing Experiment.....	23
2.2 Methods	24
2.2.1 Capsule Fabrication from Manganese Carbonate Cores	24
2.2.2 Capsule Fabrication from Melamine Formaldehyde Cores	25
3.Instrumentation	
3.1 Quartz Crystal Microbalance.....	28
3.2 Zeta Potential	30
3.3 Circular Dichroism.....	32
3.4 Atomic Force Microscopy	33
3.5 Confocal Laser Scanning Microscope	34

3.6 UV-Vis Spectroscopy	36
4. Protein Encapsulation in Thin Wall Polyion Microshells	
4.1 Introduction.....	38
4.2 Experimental Procedure.....	40
4.2.1 Microencapsulation.....	40
4.3 Instruments.....	42
4.4 Glucose Oxidase Activity Assay	42
4.5 Results and Discussion	43
4.5.1 Glucose Oxidase and Hemoglobin Encapsulation.....	43
4.5.2 Hypothesis.....	46
4.5.3 Myoglobin Encapsulation.....	49
4.5.4 Myoglobin Complexation with Open (Broken) Shells.....	50
4.6 Conclusions.....	53
5. Nanoparticles for DNA Delivery Using LbL Technique	
5.1 Introduction.....	56
5.2 Ideology/Strategy.....	58
5.3 Materials and Methods.....	60
5.3.1 Materials	60
5.3.2 Fabrication of Nanoparticles by LbL	60
5.3.3 ζ Potential Measurements and Particle Sizing	61
5.3.4 Quartz Crystal Microbalance	62
5.3.5 Atomic Force Microscopy Characterization	62
5.3.6 Cell Culture and Transfections	65
5.3.7 Confocal Microscopy	65
5.3.8 Flow Cytometry.....	66
5.4 Results	66
5.4.1 Effect of Size and Outer Coating on Cells.....	66
6. Nanoassembly of Biodegradable Microcapsules for DNA Encasing	
6.1 Introduction.....	72
6.2 Microencapsulating DNA and Characterizing.....	73
6.3 Conclusion	78
7. Conclusion	
7.1 Introduction.....	79
7.2 Nanoparticles DNA Delivery Systems	79
7.3 Microencapsulation of DNA as New Gene Vector	
References	81
Vita	88

LIST OF TABLES

Table 1.1: Protein – polyion alternate multilayer assembly	12
Table 2.1: Materials Used	20
Table 4.1: Myoglobin loading in (PSS/PAH) ₅ + PSS broken shells, pH 5 (with washing after loading at PH 8).....	51
Table 5.1: Different customized nanoparticles architecture.....	71

LIST OF FIGURES

Figure 1.1: Schematic procedure of electrostatic layer-by-layer self-assembly on plane 2-dimensional substrates and on 3-dimensional micro templates	5
Figure 1.2: LbL Self-Assembly being employed to fabricate hollow capsules.....	14
Figure 3.1: Picture of QCM instrument	29
Figure 3.2: SEM picture of a QCM electrode.....	29
Figure 3.3: Picture of Zeta Potential instrument.....	31
Figure 3.4: Picture of Zeta Potential instrument.....	34
Figure 3.5: Picture of Confocal Laser Scanning Microscope instrument.....	36
Figure 4.1: a-b Scheme of the capsule assembly and AFM image of dry 5- μm diameter (PSS/PAH) ₄ capsule.....	39
Figure 4.2: Confocal cross-sectional images of (PSS/PAH) ₄ capsules with open wall pores (at low pH) and closed pores (at high pH). FITC labeled dextran(MW70,000) was added to the solvent as fluorescent indicator	41
Figure 4.3: FITC-GOx loaded capsules: a- confocal cross-sectional image in solution at pH 8 and the fluorescent intensity profile. b – AFM tipping mode image of the dry broken capsule on mica surface.....	44
Figure 4.4: FITC-hemoglobin capsule: confocal cross-sectional image and fluorescent intensity profile of the capsule.....	44
Figure 4.5: FITC-GOx bioactivity (proportional to the absorbance increment) for the equal enzyme amount (0.007 mg/mL) free in solution (diamonds) and in the shells 15 days after encapsulation (squares), 70 and 85 days after encapsulation (red and blue)	47
Figure 4.6: UV-spectrum of encapsulated FITC-hemoglobin,ph7.5	48
Figure 4.7: Confocal cross-sectional image of FITC-Mb loaded capsules and fluorescent intensity profile of the capsule.....	49

Figure 4.8: Scheme of the two routes of myoglobin encapsulations based on pH variation for unbroken (upper route) and broken (lower route) shells.....	50
Figure 4.9: Loading of myoglobin in the shell wall depending on the protein concentration in the initial solution and on the outermost of the capsules, loading at pH 5, washing at pH 8.....	51
Figure 4.10: AFM capsule image of open-wall capsule with 3 mg/mL myoglobin loading concentration.....	53
Figure 5.1: Targeting nanoparticle Ideology/Strategy.....	58
Figure 5.2: Schematic of LbL.....	61
Figure 5.3: Charge measurement of LbL assembly through Zeta.....	61
Figure 5.4: QCM Characterization of LbL assembly.....	62
Figure 5.5: 100 nm size range nanoparticles characterized by AFM.....	63
Figure 5.6: 300 nm range nanoparticles characterized by AFM.....	64
Figure 5.7: Agglomerates of several nanoparticles thereby increasing the size characterized by AFM.....	64
Figure 5.8: AFM picture indicating different shapes and size of nanoparticles.....	65
Figure 5.9: Effect of Size on GALA Coated, Nanoparticle.....	68
Figure 5.10: Effect of Size on Lipid Coated, Nanoparticle.....	68
Figure 6.1: Schematic illustration of the DNA encapsulation process. A-B: controlled precipitation of DNA/Sperimidine (Sp) complex on the surface of template particles; B-C: LbL assembly of protective biocompatible shell; C-D: template dissolution; D-E DNA/Sp complex dissolution.....	75
Figure 6.2: Fluorescence confocal microscopy images of the DNA-containing capsules composed of 4 PA/PG bilayers just after decomposition of template core (A) and after dissolution of the inner DNA/Sp complex(B). Areas under the curves are similar. The inset demonstrates the fluorescence profile for both cases.....	76
Figure 6.3: Circular dichroism spectra of initial DNA (1); DNA captured in capsule volume (2); DNA in 0.1 M HCl (3).....	77

ACKNOWLEDGMENTS

I would like to express my appreciation to the people who have contributed their time and energy towards this project. I also would like to acknowledge my advisor Dr Yuri Lvov, whose helpful guidance and counsel have been a constant source of inspiration. I am especially indebted to for his help and concern. It was my privilege to be working under him towards my PhD degree. I would also like to extend my thankful note to Dr James Leary and Dr Tarl Prow from University of Texas Medical Branch Galveston, Texas for all the collaboration work done during the NASA project. I am thankful to the other members of the committee Dr. Michael McShane, Dr James Palmer, Dr Bill Elmore and Dr Cheng Luo for their guidance and support. During my course of study and research my advisory committee was always there to help me.

I dedicate my Dissertation to my wonderful wife Ekta Patel who always encouraged me and comforted me during my education and my life journey as well as to my family in Gujarat, India for their everlasting love and support.

I would also like to acknowledge IFM Faculty and Staff for their help and support. Last but not the least I would like to express thanks to all my colleagues from Nanofabrication Labs as well as from Biominds Lab who assisted me in times of need. Without the help and support of the people connected to me it would not be possible to complete this research.

Amish Patel

CHAPTER 1

INTRODUCTION

1.1 Nanotechnology: Nano-organized Thin Films

Nanotechnology has the ability to do things on the atomic and molecular scale. Nanotechnology is defined on the scale as being between 0.1 and 100 nanometers, a nanometer being one thousandth of a micron (micrometer), which is itself one-thousandth of a millimeter. It involves control of materials at scales from the 0.1nm up to 100nm or sometimes even higher, encompassing both ultra-miniaturization and molecular manufacturing. The beauty of working at such a scale is that each individual molecule has its own property, and exploiting such properties is not only becoming fascinating but also necessary. Nanotechnology is also a multidisciplinary branch where it encompasses scientists from physics, chemistry, biology and various other specialized fields. The opportunities for sharing skills and methods, and for joint research, seem endless in nanotechnology. It is not always easy to define nanotechnology's boundaries. Many technologies and areas of scientific research, especially in the biological sciences and biotechnology, are being reclassified as nanotechnology.

In this era, organized macromolecular and nanoparticle films are gaining importance. Thin film science and technology plays an important role in the high-tech industries and have claimed to be in the environment since last 30 years, but real exploitation of the

novel films and its properties for several multidisciplinary applications has occurred most recently. Thin films are of great importance to many real-world solutions. The cost of the material is very less as compared with the corresponding bulk material, yet they have same functionality when it comes to surface processes. Thus, knowledge and determination of the nature, functions and new properties of thin films can be used for the development of new technologies for future applications. By synthesizing specific functionalities into the polymers, the thin monolayer films can be given specific functional and performance characteristics useful in a variety of applications. In some cases, the polymers are better used in thicker films. For these applications, polymer electrolyte complexes incorporating the same polymer systems are used. Thin films can be deposited not only on bulk substrates but also onto micro- and nano-templates such as latex nanoparticles. Features such as the composition (at the surface, interior and interface of the films), thickness, uniformity, defects, contamination, interface roughness and bonding, and functionality all can be critically important depending on the film or coatings application. The mechanical properties of thin films can vary over wide ranges, depending on their dimensionality, the method of their manufacture, their pre- and post-patterning thermal history, and the constraints imposed by the materials in which they are embedded. The mechanical properties affect not only their properties and performance, but also their long-term reliability. Management of thin film is becoming increasingly important in process and device design for optimum performance and reliability. It is the understanding of the fundamental behavior of thinfilm properties that facilitates sound design of the micro- and nano-systems applications. The application of thin polymer film materials are conducting polymers, light-emitting polymers, piezoelectric polymer films,

nonlinear optical materials, nanoscale electronic circuits, protective coatings and electromagnetic shielding, pharmaceuticals, surface modifications, communication, optical electronics, catalysis, and many more. Various methods exist for ordered ultrathin nanofilms that offer various degrees of molecular order and stability, for example, spin coating, thermal deposition, the Langmuir Blodgett technique, etc. Free standing liquid crystalline films offer a very ordered structure but are very unstable. The Langmuir-Blodgett technique allows the use of planer surfaces only and cannot be applied on large areas. The disadvantages associated with LB films are that they can be used only on small and flat surfaces, and the films made with this technique also have some intrinsic defects at lipid grain borders. Another method that can be applied to surface modification is monolayer self-assembly, based on thiol or silane compounds. By this method, one can achieve self-assembly of 2 to 5 nm thick monolayer on silicon or gold surfaces, but there is no simple means to assemble thicker films with this approach. Other widely used methods for the industrial manufacture of thin films are spin coating and thermal deposition of macromolecules onto a substrate. Unfortunately, unlike the methods considered above, these methods do not allow control of the molecular order in the films. In the last decade the Layer-by-Layer Self Assembly technique (LbL) has received considerable attention for its simplicity and versatility. In nanotechnology, devices are fabricated on the sub-micron and nano scale which can be accomplished by manipulating atoms or molecules as well as overcoming the drawbacks of all previous techniques discussed. The optimal combination of molecular order and stability of films determines the practical usefulness of these technologies.

1.2 Layer-by-Layer Self-Assembly Technique

Layer-by-Layer self-assembly technique by alternate adsorption of charged macromolecules provides a molecular architecture in the direction perpendicular to the solid substrate [2-9].

This LbL technique can be employed to make ultrathin organized films in a predetermined architecture with a precision of nanometers. This technique has achieved considerable attention from the past decade mainly because of its simplicity and versatility. Layer-by-Layer self-assembly has been employed to make thin multilayers of polymers [5-15], dyes [16-19], nanoparticles (metallic, semi conducting, magnetic, and insulating) and clay nanoparticles [20-27], proteins, enzymes [28-32], and other supramolecular species on virtually any substrate.

Practically all species that have charge can be used for this technique without modifications, also any of these species in any order can be adsorbed through this technique is the greatest advantage. There is no limitation to the number of charged species that could be used in one single application. The principle of alternate adsorption was invented for charged colloidal particles and proteins in 1966 in the pioneering work of Iler [2]. Fromherz proposed the idea to assemble multilayers by alternate adsorption of charged proteins and linear polyions, but he did not demonstrate experimental results. In 1991, Decher and co-workers introduced a related method for film assembly by means of alternate adsorption of linear polycations and polyanions, or bipolar amphiphiles [3-12]. In this method the crucial feature is excessive adsorption (more than neutralization) at every stage of polycation / polyanion assembly that leads to recharging of the outermost surface at every step of film orientation.

1.2.1 L-b-L Self Assembly as Applied to Flat Surfaces

Fig. 1.1 illustrates the process of LbL self-assembly on flat support. The method provides the possibility of designing ultrathin multilayer films with a precision better than one nanometer and with defined molecular composition. The assembly procedure is briefly shown in figure above. The 2-D application is discussed which was further elaborated on the 3-D, because the same working principle is used.

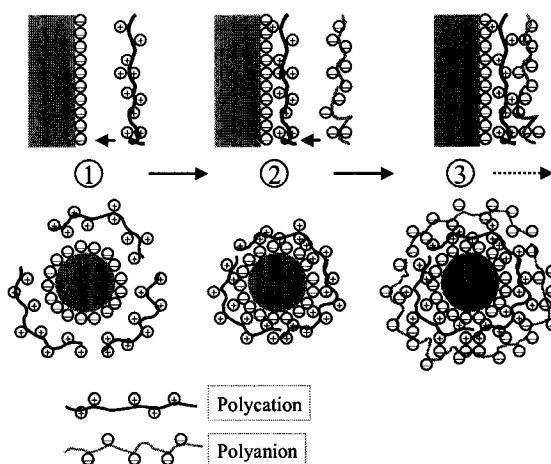


Figure. 1. 1 Schematic procedure of electrostatic layer-by-layer self-assembly on plane 2-dimentional substrates and on 3-dimensional microtemplates

A solid support (e.g., slide) with negative surface charge is incubated in the solution containing the cationic polyelectrolytes, and a layer of polycation is adsorbed. Since the adsorption is carried out at a relatively high concentration of polyelectrolytes, a number of ionic groups remain exposed at the interface with the solution, and thus the surface charge is effectively reversed. The reversed surface charge prevents further polyion adsorption. Solid supports are then rinsed with pure water to remove excess free polyions. To wash a sample use a solution of pH which keeps polyions ionized. It was shown [33] that 1 - 2 min intermediate sample water-washing (between subsequent

adsorption cycles) removes 10 - 15 % of weakly attached material from a resaturated polyion layer. This fact explains why the step of alternate polyion assembly is precise: It is not of a big importance that during one cycle we have deposited 90 % or 99 % of a saturated layer. An intermediate washing will bring them both to the level intrinsic for the assembly process parameters. The importances of intermediate washing were analyzed [34] and further dry the sample in a nitrogen stream during alternate assembly. The surface is then immersed in a solution of anionic polyelectrolytes. Again a layer is adsorbed, but now the original surface charge (negative) is restored and the surface is ready for further assembly. These two steps are repeated until a layer of the desired thickness is obtained. More than two components can be used in the assembly with the only condition: a proper alternation of positive and negative compounds. The forces between components and binder layers govern the spontaneous layer-by-layer self-assembly of ultrathin films. These forces are primarily electrostatic and covalent, but they can also involve hydrogen bonding, hydrophobic, and other types of interactions. That any of these species in any order can be adsorbed layers is the greatest advantage of self-assembly. The oppositely charged species are held tighter by strong ionic bonds, and they form long-lasting, uniform, and stable films. Self-assembly is economical and readily amenable to scaling up for the fabrication of large-area defect-free devices on any kind and shape of surface. For observation of the assembly growth on the flat substrate the most commonly used tool is the quartz crystal microbalance [18, 21, 33, 35].

The kinetics of the adsorption process could be delineated by the QCM technique; this technique is indispensable for establishing proper assembly conditions (a saturation adsorption time). One does not need to maintain an adsorption time with great precision;

a minute more or less does not influence the layer thickness if we are at the saturation region.

1.2.2 L-b-L Self Assembly as Applied to Colloids

Similarly ordered multilayers can be deposited on colloids (Fig. 1.1), i.e., organic and inorganic particles. The procedure is similar for 2-D as well as 3-D. The only major difference is now that the assembly is occurring on the core particles so that the excess of polyions after deposition will be removed by washing in proper media through centrifuge. The centrifugation speed is varying according to the size of the core particles, and after every polyelectrolyte layers deposited three washes will be given to the system in the appropriate media. Number of core particles can be used to the extent that they are charged system.

The main idea of the method consists of the resaturation of polyion adsorption, resulting in the alternation of the terminal charge after every subsequent layer deposition. This idea is general and implies that there is no principle restriction to the choice of polyelectrolytes as well as core systems. For the successful assembly of nanoparticles or protein multilayers, the alternation with linear polyion layers is important. Flexible linear polyions penetrate between nanoparticles and enzymes and act as electrostatic glue. The self-assembled film contains amorphous polyion interlayer, and this organization heals defects that arise as a result of the introduction of foreign particles (dust, microbes) during the process of film formation. [13, 30]

The thickness may also be controlled by introducing internal layers which indeed will be providing potential application in the field of drug delivery systems or in diagnostics,

where the particles can be directed by application of external magnetic fields, [36] and in turn variation of salt concentration could be very effective for the thickness and bonding of the polyelectrolyte [37]. The ionic and hydrophobic polyanion polycation nanoparticles surface charge, created by the adsorption of anions interactions which are insufficient, can also be immobilized by covalently attaching an anion thiol before polyelectrolyte [37]. The polyelectrolyte multilayer film formed through electrostatic force of attraction due to its different molecular density can allow selective permeation and give a cutoff to certain specific species. The advantage posed by the polyelectrolyte multilayer film is that the porosity of the surface charge can be controlled arbitrarily by changing the type of polyelectrolyte in the outermost layer, in turn leading to the application of sensors. [38] Various methods such as adsorption of the polyelectrolytes at a concentration exceeding saturation amount was combined with removal of the non bound polyelectrolytes using centrifugation and adsorption of polyelectrolytes with concentration just sufficient for saturation coverage has been employed for multilayer growth, resulting in a continuous layer growth. [39] This technique also enables the arrangement of the optically active molecules or chemically active functional groups at molecular level, to produce cooperative electronic and optical properties including electro luminescence, [40-42] second harmonic generation, [43] and photon induced electron transfer. [44]

1.3 Basics of Thin Film Adsorption

We are not investigating the chemical kinetics of the films formed using the LbL technique, but a brief overview is given based on the previous research works. For the time-dependent control of adsorption and monitoring of the assembly *in situ*, the quartz

crystal microbalance (QCM) method is very well known and suitable [15,34]. The kinetics of the adsorption process can be explained by the QCM technique, which is essential for establishing proper assembly conditions. The multilayer assemblies are characterized by means of the QCM technique in two ways:

1. Drying a sample in a nitrogen stream, we measured the resonance frequency shift and calculated an adsorbed mass by the Sauerbrey equation; this approach is very simple and most commonly used phenomenon.
2. Monitor the resonator frequency during adsorption onto one side of the resonator, which was in permanent contact with polyion solution. While performing experiments in permanent contact with polyion solution, touching the surface of solution with one side of the resonator while the upper electrode was kept open to the air. The upper contact wire is insulated from the solution by a silicone paint covering.

Generally, in most publications on polyion assembly, adsorption times of 4 to 15 min are used as discussed above that, and once saturation region of assembly is reached, time does not matter. Polyion films swell by 50% before drying, but only 5-10% of the water remains in polyion films after drying. The high hydration of adsorbed polyions (≈ 50 wt %) as compared with the dried film was measured in solution by the light-guiding attenuation technique [24]. Polyion adsorption occurs in two stages: quick anchoring to a surface and slow relaxation. To reach a surface charge reversion during linear polyion adsorption one needs a concentration greater than 10^{-5} M [45].

The dependence of polyion layer thickness on concentration is not great: thus, over the concentration range of 0.1-5 mg/mL, a PSS-PAH pair yielded similar bilayer thickness. A further decrease in polyion concentration (using 0.01 mg/mL) decreases the layer

thickness of the adsorbed polyion. An increase in the component concentrations to 20-30 mg/mL may result in nonlinear growth rate with successive adsorption steps, especially if an intermediate sample rinsing is not long enough [46]. Most of the time the concentration used for forming films in the cited publications is below 6 mg/ml.

It was proposed that in adsorption from water (at low ionic strength solutions) one deals with strongly charged polyion adsorption, which forms a well, attached monolayer. In adsorption from high ionic strength solutions (at salt concentrations of the order 0.1 - 1.0 M) one has partially neutralized polyion chains, which provide adsorption with major loops and the step of film growth becomes much greater [13]. Such results are demonstrated by poly(dimethyldiallylammonium chloride) / poly(styrenesulfonate) (PDDA/PSS) alternate adsorption from solutions with different ionic strength resulting in the bilayers growth step variation from 1.6 nm up to 6 nm.

The polycation / polyanion bilayers thickness depends on the charge density of the polyions. It was shown that more than 10 % of polyion side groups have to be ionized for a stable reproducible multilayer assembly via alternate electrostatic adsorption [34].

High ionization of polyions results in a smaller step of film growth (1 - 2 nm) and lower ionization gives a larger growth step (3 - 6 nm). It can be reached either by adding salt to a polyion solution (as discussed above for strong polyelectrolytes, such as PDDA and PSS), or by varying the pH for weak polyelectrolytes (e.g., polyacrylic acid (PAA) and poly(allylamine) (PAH), as was analyzed recently by Rubner et al [47].

One other phenomenon generally seen in adsorption of films on the substrate is the nonlinear growth of the films on substrates [13, 46]. For the first two or three layers, smaller amount of polyion are adsorbed than during further assembly, when the film mass

and thickness increase linearly with the number of adsorption cycles. Tsukruk *et al.* [46] explained this effect as an island-type adsorption of the first polyanion layers on a weakly charged support. In the following two or three adsorption cycles these islands spread and cover the entire surface, and further multilayer growth occurs linearly. If a substrate is well charged, then the linear growth with successive steps begins earlier. In studying the possibility of using new compounds in the assembly, a precursor film approach [6, 13, 46] is generally used. Normally repeating two or three alternate adsorptions of PEI and PSS assembles the precursor films. The outermost layer became negative or positive, respectively depending on the next layer employed. Some common instruments used for characterizing the growth of films on the substrates are Surface Contact Angle & UV-Vis.

1.3.1 Protein Films

The films from proteins have multiple applications and it is very important to preserve their activity once the proteins are embedded in the layers. To date several proteins have been used and characterized in films and mostly with positively charged PEI, PAH, PDDA, or with negatively charged PSS, DNA, or heparin. [14, 23, 48-55].

The proteins are active in the films and thus it attracts the scientists to use them. The pH of the protein solutions is kept away from the isoelectric point so that the proteins are sufficiently charged under the experimental conditions. The assembly of 20 different proteins was successfully achieved as shown in the table (including cytochrome, carbonic anhydrase, myoglobin, hemoglobin, bacteriorhodopsin, pepsin, peroxidase, alcohol dehydrogenase, glucoamylase, glucose oxidase, immunoglobulin, catalase, and urease (Table I) [56]. All the proteins underwent the alternate adsorption with organic polyanions

for unlimited numbers of cycles. The mass increment at each step was quite reproducible. Proteins immobilized in multilayers with strong polyions such as PSS, PEI, and PDDA were insoluble in buffer over a pH range between 3 and 10. The assembled proteins are in most cases not denatured [29, 32, 57, 58]. Moreover, in some case the L-B-L immobilization with linear or branched polyions enhanced the enzymatic stability [32].

Table 1.1 Protein – polyion alternate multilayer assembly [56]

Protein	Molecular Weight	Isoelectric Point	pH used	Charge	Alternate With	Protein	Thickness
						Mass Coverage (mg/m ²)	Monolayer of protein +polyion bilayer (nm)
Cytochrome c	12400	10.1	4.5	+	PSS ⁻	3.6	2.4 + 1.6
Lysozyme	14000	11	4	+	PSS ⁻	3.5	2.3 + 1.9
Histone f3	15300	11	7	+	PSS ⁻	3.3	2.2 + 2.0
Bacteriorhodopsin	26000	6	9.4	-	PDDA ⁺	7.5	5.0 + 1.0
Pepsin	35000	1	6	-		4.5	3.0 + 0.6
Peroxidase	42000	8.0	4.2	+	PSS ⁻	5.3	3.5
Albumin	68000	4.9	8	-	PDDA ⁺	23	16.0 + 1.0
			3.9	+	Heparin ⁻		20.0 + 1.0
Glucoamylase	95000	4.2	6.8	-	PDDA ⁺ , PEI ⁺	30	2.6 + 0.5
Photosynt. RC	100000	5.5	8	-	PDDA ⁺	4	9.0 + 1.0

Concanavalin	104000	5	7	–	PEI ⁺	8.6	5.7 + 0.8
Alcohol dehydrogenase	141000	5.4	8.5	–	PDDA ⁺	12.2	8.5 + 1.0
IgG [72]	150000	6.8	7.5	–	PSS ⁻	15	10.0
Glucose oxidase	186000	4.1	6.8	–	PDDA ⁺	12	8.0
			6.5	–	PEI ⁺	51	34.4 + 0.8
Catalase	240000	5.5	9.2	–	PEI ⁺	9.6	6.4 + 0.8

1.4 Formation of Capsules

Several applications of thin films have been mentioned; also the limitless species used for the LbL assembly renders the opportunity to grow films for the suited applications. The concept of growing films on the colloidal systems has been elaborated further by choosing the core systems that can be dissolved under suitable condition without any damage to the films grown. Thus, much attention has been paid not only to the elaboration of microencapsulation technologies but also to designing the polymer/protein coatings with the pre-determined and controllable physicochemical properties, which can be of help during dissolution of core without any damages to the wall texture. Preserving the wall texture is one of very important issue that should be kept during the dissolution of the core as once the core is dissolved the walls render their applicability for further use. Various colloidal templates organic and inorganic such as MF particles (most commonly used), organic crystals, [59] carbonate particles [60] and biological cells are used for hollow capsule fabrication.

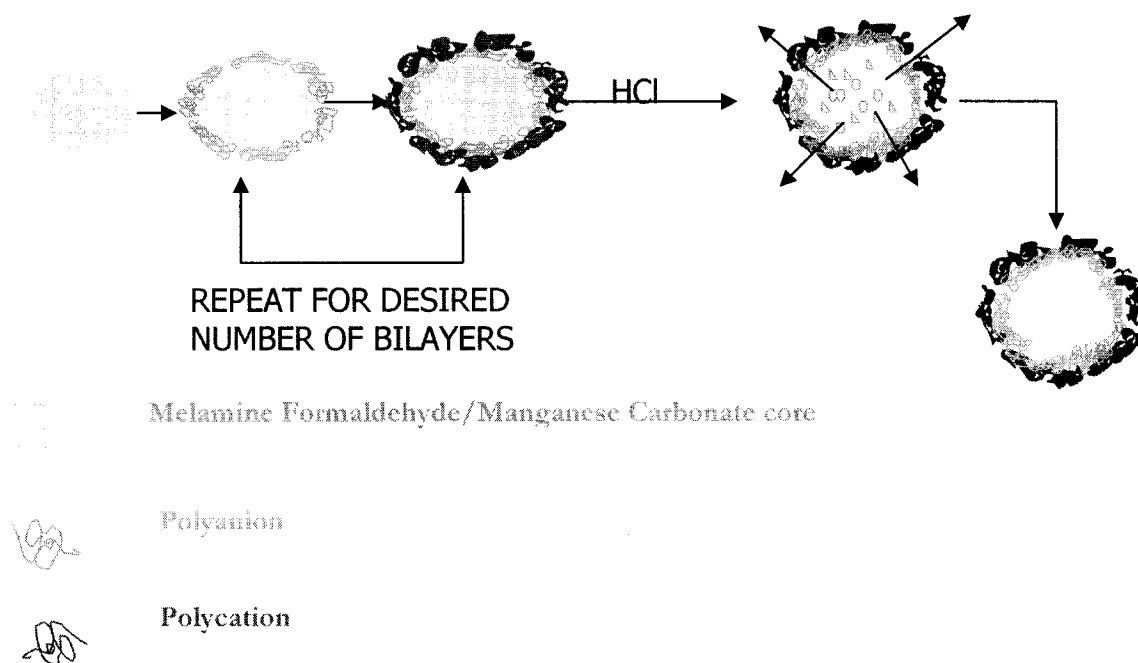


Figure. 1.2 LbL Self-Assembly being employed to fabricate hollow capsules

Hollow capsules can be fabricated by dissolving the core at low pH for MF particles and carbonate particles, organic water-miscible solvents for organic crystals, and the strong oxidizing agents (NaOCL) for biological cells. The dissolution of core has been intensely studied on the MF particles, which have been dissolved by 1M NaCL and in some water-miscible solvents DMF or DMSO at lower Ph HCL (Ph<1.2). Today the MF cores are been replaced by Carbonate cores because of the residues of MF after dissolution in most cases. The core to be used is based on the application and the polyelectrolyte used; thus, the dissolution of the core should not have an effect on the wall texture. The hollow polyelectrolyte capsules with diameter varying from .2 to 10 microns and wall thickness from few to tens of nanometer are obtained. The size of the template determines the diameter of the hollow capsule. The characterization of the hollow polyelectrolyte microcapsules fabrication can be done with the help of scanning transmission, atomic force microscopy, and confocal fluorescent microscopy.

1.4.1 Encapsulation

A new approach to the microencapsulation as an extension of the “layer-by-layer electrostatic self-assembly” of different materials, based on alternating adsorption of oppositely charged polyelectrolytes onto colloid-sized microparticles, has been put forward and is now recognized as simple but extremely versatile for designing nanocomposite multilayered polyelectrolyte film [3, 61-65]. The properties of flat polyelectrolyte films of microcapsules include the permeability of the walls, which can be controlled by various possible combinations of different polyelectrolyte pairs, other charged entities, purposeful chemical modification of starting materials, and unique alternating packing of positively and negatively charged polyelectrolyte layers. The release of the encapsulated core substances into surroundings is achieved either by direct disruption of polymeric shells in some way, for instance, mechanical, chemical, biological degradation, the exposure to physical factors like heat, electromagnetic irradiation of different wavelength and others or even by subtle management of the permeability of microcapsules walls with retaining their overall integrity. When one introduces magnetic materials in the shell composition, the release of the encapsulated particle can be manipulated by applying external magnetic field [25, 66]. After the formation of the hollow microshell the encapsulation is based on the semipermeable properties of the polyelectrolyte capsule walls. The permeability of the wall allows only low molecular weight such as dyes and ions leaving the higher molecular weight [67]. Researchers are showing a keen interest in switching and controlling capsule permeability for macromolecules [68]. One possible approach to load capsules with polymers is to desorb polyelectrolytes from inner layers of empty shells into their

interior. This technique has several limitations with regard to the polymer species and the accompanying harsh conditions, such as low pH, oxidizing agents or organic solvents, which are used for core decomposition [69]. This technique has an appealing application in the different areas of technology, such as catalysis, cosmetics, medicine, biotechnology, nutrition, and so on. The properties and structure of the polyelectrolyte multilayers are sensitive to a variety of physical and chemical conditions of the surrounding media which might dramatically influence on structure of polyelectrolyte complexes and result on permeability of the capsules. One of the main influences in the opening and closing of the polyelectrolyte walls is governed by change in pH. Upon variation of the pH, the change in the polyelectrolyte charge induces pore formation of about 50-200nm or loosening the polyelectrolyte network, which enables the polymer penetration [70]. The behavior of the polyelectrolyte layers can be made undeformable to a certain extent by adding lipids. The addition of the lipids to the microcapsule results in remarkable change in the mechanical properties to the capsule walls. Thus the variation of the polyelectrolyte can have a great influence on permeability of molecular species. Much of encapsulation research today also involves the study of substances called polymers, chemically manufactured gel-like materials that scientists are using to surround or encapsulate cells. The properties of the core can be enhanced by pre-charging later on monitoring the fluorescence to get the information on transport process in the ultrathin films of polyelectrolytes emitted during the dissolution of the core, when exposed to solvent which in turn will influence the capsule porosity for encapsulation of uncharged low molecular weight organic materials [63, 71].

Various theoretical models based on several assumptions like permeability of the capsule wall, charging of the capsule and osmotic balance of the loaded capsule with small ions and capsule suspended in the bulk solution also help to prove the variation of the pH and change in the surrounding composition leads to encapsulation [72], also varying the pH of the surrounding the permeability of the hollow capsule wall can be controlled. The pH in the interior of the hollow polyelectrolyte capsules and the exterior of the hollow polyelectrolyte can be kept different as a result of which different solvents can be filled in the capsules [73]. The loaded material conjugated with the fluorescence dye can be monitored using confocal microscopy, to check the encapsulation stability. This is one of the most common methods used today for characterizing encapsulated species. The quantization of the loaded dye can be made with the help of Spectrofluorometer as the emission intensity of the light is directly proportional to the concentration of the analyte. The encapsulation of the enzymes in the microshell, through the opening and closing of the pores can be a well known application as a micro and nanoreactor [72]. Taking one step ahead in the field of loading, researchers have started conjugating the polyelectrolytes and along with the encapsulating materials. Spectrofluorometer and Confocal Microscopy are quite famous and most commonly used instruments for characterizing loading as well as properties of encapsulated materials.

1.5 Ideology

1.5.1 Protein Loading

Thin wall microcapsules were formed via a layer-by-layer self-assembly by eight-ten steps of alternate adsorption of oppositely charged poly(styrenesulfonate) and poly(allylamine) on microcores. After the core dissolution, empty polymeric shells with 20-25 nm thick walls were obtained. These microcapsules were loaded with myoglobin, hemoglobin and glucose oxidase by opening capsule pores at low pH and closing them at higher pH.

1.5.2 Nanoparticles for DNA Delivery Using LbL Technique

The above concept of assembly on core particles was employed for one of our projects, Gene Therapy where we are layering core particles of silica with species of interest such as DNA, Targeting Moieties and many others. Such assembly will help to design the films on the core particle system, which can further be employed for targeting a specific site based on the receptor systems. The films on the core particle system will carry payloads of required species to be delivered at a specific site. This technique is also been developed for some bioassays where manufacturers use a fluorescence polystyrene beads that can be further coupled to antibody, proteins, peptide to target the receptor. Such technique is already been developed by Luminex Technologies, Austin and is known as XMAP technologies.

1.5.3 DNA Encasing

The concept of LbL is used to encapsulate DNA in biocompatible shells. This is a novel delivery approach where further design of small vectors can be done to help deliver DNA to the specific targets. This designed experiment helped to construct biocompatible coatings shells that encased the DNA and protected its native structure.

CHAPTER 2

MATERIALS & METHODS

2.1 Materials

Several different materials are used in the experiments and some of the major used materials are given in the table below. The concentration of solution ranges normally around 2 mg/ml to 5 mg/ml. The materials were used on the bases of the application and the iso electric point.

Table 2.1 Materials Used

Materials Used	MW gm/mole
poly(styrenesulfonate) (PSS)	70,000
poly(allylamine) hydrochloride (PAH)	50,000
Poly(ethylene imine) (PEI)	2,000
glucose oxidase	186,000
bovine hemoglobin	64,000
myoglobin	17,800
D-Galactosamine Hydrochloride (gala)	294
chondroitin sulfate (PG)	45,000-70,000
poly(-L-arginine)	14,000

sperimidine	254
protamine sulfate	5120
pegfp DNA	4903800
DNA calf thymus	10-15 million

2.1.1 Protein Loading Experiments

Hollow polyelectrolyte capsules were fabricated at pH 6.5, 0.5 NaCl by alternate adsorption of four bilayers of sodium poly(styrenesulfonate) (PSS) (Aldrich, MW 70,000) / poly(allylamine) hydrochloride (PAH) (Aldrich, MW 50,000), onto 5- μ m diameter melamine formaldehyde (MF) particles (Microparticles GmbH, Berlin). For the multilayer shell formation, $\sim 10^{11}$ core particles were added to a 2-mL Eppendorf centrifuge tube followed by the addition of polyions to give shell architectures of the following sequence: (PSS/PAH)₄₋₆.

For loading, 0.2 mL of capsules and 0.2 ml of proteins with concentration 2 mg/ml were incubated at pH 6 for 20 min. Then pH of solution was adjusted to pH 10 and remaining proteins were washed out three times with 2 mL water and centrifugation, so that final pH = 8. Glucose oxidase, bovine hemoglobin and myoglobin (all from Sigma) were used without further purification. These proteins were labeled with fluorescein isothiocyanate (FITC) (Sigma) by incubation with the marker (mass ratio protein / FITC was 30/1) in pH 9 boric buffers for 3 hours at room temperature. Confocal Microscopy was used to characterize loading.

2.1.2 Nanoparticles for DNA Delivery Experiments

Nanoparticles were constructed by using a charged 78 nm silica particles as cores. (Nissan Chemical, Inc.). Using Layer-by-Layer Self-Assembly technique alternate charged layers were deposited of polyethylimine, DNA, sugars, and proteins depending on their charge (Sigma-Aldrich Chemical, Inc). Deposition of each layer was monitored through sizing and zeta potential with a ZetaPlus (New Haven Instruments, Inc.) Atomic Force Microscopy was also used for sizing the nanoparticles. DNA, including pEGFP-C1 and pdsRed-2 were initially obtained from Clontech, Inc. Quantities of DNA were obtained from transforming specific E. coli with the appropriate plasmid and growing them. The bacteria were lysed and the DNA isolated through cesium chloride gradients. All DNA were then concentrated and kept frozen in water. Linear DNA was obtained by large scale PCR reactions using the above plasmids as templates. After the PCR reactions, the resulting DNA was isolated using commercial PCR product purification kits provided by Qiagen, Inc. The DNA after preparation or direct purchase was sent to Louisiana Tech University for the experiments from University of Texas Medical Branch, Galveston, Texas. The outer coatings included galactosamine, protamine, and poly-arginine, bovine serum albumin purchased from Sigma-Aldrich, Inc. Lipid coatings were deposited on DNA coated nanoparticles just before exposure to cells. Lipofectamine 2000 was used to coat the nanoparticles in a method identical for DNA transfections as directed by the manufacture instructions. Once the non viral vectors were prepared they were send to UTMB for further experiments with cells. Cells were incubated at 37C in 5% CO₂. Huh-7 and HeLa cell lines were cultured in DMEM supplemented with 10% FBS (Sigma, Inc.) and Penicillin/Streptomycin (Sigma, Inc.). Cells were transiently

transfected with Lipofectamine2000 (Invitrogen, Inc.) using the manufacturer's instructions. Each experiment was done at least in triplicate.

2.1.3 DNA Encasing Experiment

MnCO₃ particles of 4 μm diameter (from PlasmaChem GmbH) were taken as template cores. A 0.5 mg/mL MnCO₃ particle suspension (30 ml) was mixed with 1 mL of 1.5 mg/mL DNA solution (highly-polymerized DNA sodium salt from Calf Thymus, Sigma). Precipitation of DNA/Sp complex on template particles was made adding dropwise 2 mL of 1 mg/mL spermidine solution into stirred MnCO₃/DNA solution. Further alternated LbL assembly of biocompatible poly[β-glucuronic acid-(1→3)-N-acetyl-β-galactosamine-6-sulfate-(1→4)] (known as chondroitin sulfate, Sigma) (PG) / poly(-L-arginine) (PA) shell was carried out with 1 mg/mL PA or PG solutions. After each deposition step, microparticles were washed out 3 times. A layer-by-layer assembly of polyelectrolyte layers was monitored by electrophoretic mobility measurements (ZetaPlus Zeta Potential Analyzer, Brookhaven Instr. Corp). 5 nm assembly steps for PA/PG were found from parallel PA/PG assembly on QCM electrode (Quartz Crystal Microbalance, USI-System, Japan). Therefore, a total capsule wall thickness was 40 nm. Further DNA was also labeled with Rhodamine dye for characterization of loading through confocal microscope. Circular dichroism was also used to monitor the structure of the encapsulated DNA.

2.2 Methods

2.2.1 Capsule Fabrication from Manganese Carbonate Cores

The fabrication of capsules is as follows:

- Manganese Carbonate particles with concentration of 10mg/20 ml is taken and sonicated for 5 minutes.
- Once sonicated the particles are allowed to sediment, excess of water is thereafter removed and the particles with 2ml suspension are transferred to a vial.
- The mixture is centrifuged for 4 min at 3000 rpm.
- The supernatant is removed, and the particles are suspended in the polyanion solution until the 2ml mark (in this case as the substrate is positively charged the polyelectrolyte used is negatively charged).
- The suspension is allowed to settle for 15 min.
- It is centrifuged at 3000 rpm for 4 min.
- The supernatant is removed and water/buffer is added, centrifuged at 3000 rpm for 4 min.
- Three washes of water/buffer are treated to make sure that no polyanion other than attached is left in the vial.
- After 3 treatment of water/buffer, the polycation solution is added and the particles are uniformly suspended with the help of vortex and sonicator. The suspension is allowed to settle for 15 min.
- Then it is centrifuged for 4 min at 3000 rpm.
- The supernatant is removed, and three washes of the resultant particles with layers of polyanion are washed with water/buffer. This washing removes excess of polyanions.
- Repeat the above steps for desired number of layers.

After the assembly of the desired number of layers the formation of hollow capsules is the next step in the experiment. The shells treated with the three-water/buffer washes are kept in the vials after the removal of supernatant.

- HCl of pH < 1.1 is added to the vial. As acid is added, the solution becomes clear which indicates that dissolution is taking place. The cores can also be dissolved by adding EDTA (EthyleneDiamineTetraAcetic acid dehydrate) solution and keeping it overnight.
- Due to sensitivity of the hollow capsule wall to low pH conditions, the acidic solution is removed via centrifugation at 5500 rpm for 15 minutes.
- Six washes of water/buffer are treated to remove and make sure that acid is removed completely.

2.2.2 Capsule Fabrication from Melamine Formaldehyde Cores

The fabrication of shells is as follows:

- Vial of 2 ml capacity is rinsed with de-ionized water and dried using a nitrogen gun.
- MF particles in the range of 100 to 150 μ l are taken in the vial.
- Tris-buffer solution is added to the vial till 2 ml mark, and the mixture is vortexed or sonicated for proper suspension.
- The mixture is centrifuged for 5 min at 6000 rpm.
- The supernatant is removed and the MF particles are suspended in the polyanion solution till the 2ml mark (in this case as the substrate is positively charged the polyelectrolyte used is negatively charged).
- The suspension is allowed to settle for 15 min.
- It is centrifuged at 6000 rpm for 5 min.

- The supernatant is removed, and tris buffer is added, centrifuged at 6000 rpm for 5 min.
- Three washes of tris buffer are treated to make sure that no polyanion other than attached is left in the vial.
- After 3 treatment of tris-buffer, the polycation solution is added and the particles are uniformly suspended with the help of vortex and sonicator. The suspension is allowed to settle for 15 min.
- Then it is centrifuged for 5 min at 6000 rpm.
- The supernatant is removed and three washes of the resultant particles with layer of polyion are washed with tris buffer. This washing removes excess of polyions. The centrifugation specifications are 6000 rpm for 5 min.
- Repeat the above steps for desired number of layers.

After the assembly of desired number of layers the formation of hollow capsules is the next step in the experiment. The shells treated with the three tris buffer washes are kept in the vials after the removal of supernatant.

- HCl of pH < 1.1 is added to the vial. As acid is added the solution becomes clear which indicates that dissolution is taking place.
- Due to sensitivity of the hollow capsule wall to low pH conditions, the acidic solution is removed via centrifugation at 5000 rpm for 10 minutes.
- Six washes of tris buffer are treated to remove the acid completely.

Thus hollow microcapsules have been fabricated. After the fabrication of the hollow shells, the loading of the shells takes place. Adjusting shell permeability by changing a solvent (water-alcohol-acetone), ionic strength or pH helps loading phenomenon. For loading, 0.2 mL of capsules and 0.2 ml of proteins with concentration 2 mg/ml were

incubated at pH 6 for 20 min. Then pH of solution was adjusted to pH 10 and remaining proteins were washed out three times with 2 mL water and centrifugation, so that final pH = 8.

CHAPTER 3

INSTRUMENTATION

The most commonly used instruments for characterization of step growth of LbL assembly on flat surface is the Quartz Crystal Microbalance. Zeta Potential is used for measuring charge alteration on colloidal systems, it helps to study the deposition of the alternate polyelectrolyte layers. One of the other commonly used instrument for studying the bioactivity of the enzymes encapsulated or for performing assays of the encapsulated enzyme is UV-Vis. Circular Dichroism was also used for characterization of the native structure of the encapsulated materials. It also helps to characterize assembly on flat surfaces by measuring the absorbance after each layer deposited.

3.1 Quartz Crystal Microbalance

The Quartz Crystal Microbalance (QCM) is a very sensitive mass balance, capable of sensing mass changes within nanograms. QCM is a mass sensor. The QCM device is used to study molecular interactions and molecular adsorption to different surfaces, such as properties of biomaterials and functionalized surfaces. Applications include proteins, lipids, polyelectrolyte, polymers, polymer films and cells / bacteria. The QCM technique

determines the mass of very thin surface-bound layers. A QCM consists of a thin quartz disc sandwiched between a pair of electrodes. Due to the piezoelectric properties of quartz, it is possible to excite the crystal to oscillation by applying an AC voltage across its electrodes. Changes to this resonance are directly proportional to mass changes. If the film is thin and rigid the decrease in frequency is proportional to the mass of the film. In this way, the QCM operates as a very sensitive mass balance. The mass of the adhering layer is calculated by using the Sauerbrey relation:

$$\Delta T \text{ (nm)} \approx -(0.016 \pm 0.002) \Delta F \text{ (Hz)} \dots\dots\dots (2.1)$$

$$\Delta M \text{ (ng)} = -0.87 \Delta F \text{ (Hz)} \dots\dots\dots (2.2)$$

where ΔF is the shift of QCM frequency after each layer is deposited.

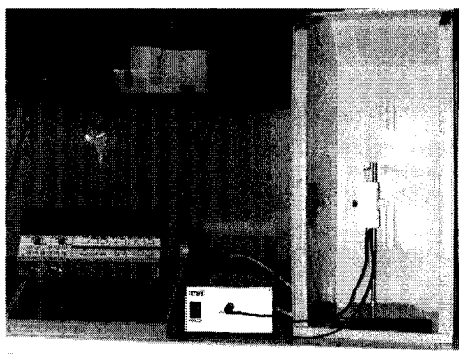


Figure 3.1: Picture of QCM instrument

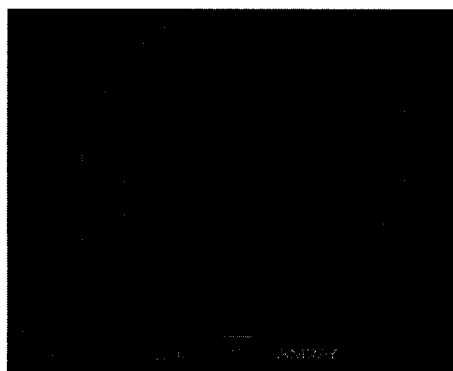


Figure 3.2: SEM picture of a QCM electrode

3.2 Zeta Potential

The zeta potential is a measure of the magnitude of the repulsion or attraction between particles. Its measurement brings detailed insight into the dispersion mechanism and is the key to electrostatic dispersion control. The measurement of zeta potential is an extremely important parameter. Zeta Potential instrument is used basically for measuring the charge of solution or colloidal system. Zeta Potential helps to monitor the growth of film on the colloidal systems. When subjected to an electric field each particle and its most closely associated ions move through the solution as a unit and the potential at the boundary between this unit i.e. at the surface of shear between the particle with its ion atmosphere and the surrounding medium, is known as the zeta potential ζ . When a layer of macromolecules, whether a polyelectrolyte or an uncharged polymer, is adsorbed on the surface of the particle, this can alter the zeta potential simply because it shifts the location of the shear plane further from the actual surface. Zeta potential is therefore a function of the surface charge of the particle, any adsorbed layer at the interface and the nature and composition of the surrounding medium in which the particle is suspended. It is usually, but not necessarily, of the same sign as the potential actually at the particle surface but unlike the surface potential, the zeta potential is readily accessible by experiment. Moreover, because it reflects the effective charge on the particles and is therefore related to the electrostatic repulsion between them, zeta potential has proven to be extremely relevant to the practical study and control of colloidal stability. The principal of determining zeta potential is very simple. A controlled electric field is applied via electrodes immersed in the sample suspension and this causes the charged particles to move towards the electrode of opposite polarity. Viscous forces acting upon

the moving particle tend to oppose this motion and equilibrium is rapidly established between the effects of the electrostatic attraction and the viscous drag. The particles therefore reach a constant "terminal" velocity. This velocity is dependent upon the electric field strength or voltage gradient, the dielectric constant and viscosity of the liquid - all of which are known - and the zeta potential. It is usually expressed as the particle mobility, which is the velocity under unit field strength. For all practical purposes, the relationship between mobility, μ , and zeta potential, ζ , is quite simple.

Helmholtz-Smoluchowski equation relates this and is given by:

$$\mu = (\zeta \epsilon) / \eta$$

Thus the measured electrophoretic mobility μ [E] is converted into the zeta-potential (ζ [mV]) by using the Helmholtz-Smoluchowski relation. The value of the zeta-potential indicates the surface charge of a particle. High absolute zeta-potentials indicate stable colloidal systems. The alternate value of zeta-potential is indicative of the successful recharging of the colloidal surface in layer-by-layer assembly.

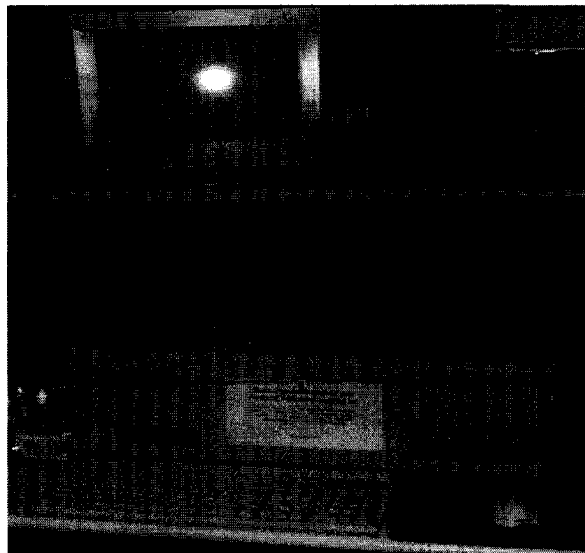


Figure 3.3: Picture of Zeta Potential instrument

3.3 Circular Dichroism

Circular Dichroism spectroscopy is particularly good for:

- Determining whether a protein is folded and if so characterizing its secondary structure, tertiary structure and the structural family to which it belongs
- Comparing the structures of a protein obtained from different sources (eg. species, or expression systems) or comparing structures for different mutants of the same proteins
- Demonstrating comparability of solution conformation after changes in manufacturing processes of formulation
- Studying the conformational stability of a protein under stress-thermal stability, pH stability, and stability to denaturants and how this stability is altered by buffer composition or addition of stabilizers
- Determining whether the protein-protein, protein-polymer interaction alter the conformation of proteins

Circular Dichroism spectroscopy is a type of absorption spectroscopy that can provide information on the structures of many types of biological macromolecules. Circular Dichroism is the difference between the absorption of left-handed and right-handed circularly polarized light and is measured as a function of wavelength. Molecules produce a circular dichroism spectrum because they absorb left-handed and right-handed polarized light to different extent and thus are considered to be optically active. Biologically macromolecules such as proteins and DNA are composed of optically active elements, and because they can adopt different three -dimensional structures each type of molecules produces distinct circular dichroism spectra. Different types of protein

secondary structures such as helices, sheets, turns, and coils give rise to different circular dichroism spectra. Due to the helical structure of double-stranded DNA, its circular dichroism (CD) spectrum has a strong signal in 230-350 nm range. This characterization helps to determine the structure of the molecule after encapsulation or exposing to hostile environment.

3.4 Atomic Force Microscopy

The Atomic Force Microscopy is being used to solve processing and materials problems in a wide range of technologies. The materials, which can be investigated, include thin and thin film coatings, ceramics, composites, glasses, polymers and many more. By using AFM one can image surface in atomic resolution and also measure force at atomic level. The atomic force microscope is one of about two dozen types of scanned-proximity probe microscopes. All these microscopes work by measuring a local property such as height, optical absorption, or magnetism with a probe or "tip" placed very close to the sample. The basic objective of the operation of the AFM is to measure the forces (at the atomic level) between a sharp probing tip (which is attached to a cantilever spring) and a sample surface. The small probe-sample separation (on the order of the instrument's resolution) makes it possible to take measurements over a small area. AFM operates by measuring attractive or repulsive forces between a tip and the sample. In its repulsive "contact" mode, the instrument lightly touches a tip of "cantilever" to the sample. As a raster-scan drags the tip over the sample, some sort of detection apparatus measures the vertical deflection of the cantilever, which indicates the local sample height. Thus, in contact mode the AFM measures repulsion forces between the tip and sample. To acquire an image, the microscope raster-scans the probe over the sample while measuring the local

property in question. The resulting image resembles an image on a television screen in that both consist of many rows or lines of information placed one above the other. The ability of AFM to image at atomic resolution, combined with its ability to image a wide variety of samples under a wide variety of conditions, has created a great deal of interest in applying it to the study of biological structures. Images have appeared in the literature showing DNA, single proteins, and living cells. This characterization helps us to understand the size dimension of the nanoparticles for DNA delivery as well as allows us to see how a hollow capsule looks like.



Figure 3.4: Picture of Atomic Force Microscopy Instrument

3.5 Confocal Laser Scanning Microscope

Confocal Laser Scanning Microscopy (CLSM) offers observation of thin optical sections in thick, intact specimens. In conventional fluorescence microscopy, out-of-focus fluorescence, evoked by the excitation light, tends to overwhelm details in the actual

image plane. In CLSM a laser light beam is expanded to make optimal use of the optics in the objective. Through a x-y deflection mechanism this beam is turned into a scanning beam, focused to a small spot by an objective lens onto a fluorescent specimen. The mixture of reflected light and emitted fluorescent light is captured by the same objective and (after conversion into a static beam by the x-y scanner device) is focused onto a photodetector (photomultiplier) via a dichroic mirror (beam splitter). The reflected light is deviated by the dichroic mirror while the emitted fluorescent light passes through in the direction of the photomultiplier. A confocal aperture (pinhole) is placed in front of the photodetector, such that the fluorescent light (not the reflected light!) from points on the specimen that are not within the focal plane (the so called out-of-focus light) where the laser beam was focused will be largely obstructed by the pinhole. In this way, out-of-focus information (both above and below the focal plane) is greatly reduced. This becomes especially important when dealing with thick specimens. The spot that is focussed on the center of the pinhole is often referred to as the "confocal spot." CLSM is a powerful tool for three-dimensional (3D) analysis of fluorescently labelled specimens. This instrument is a very important for characterizing whereby one can conjugate fluorescent labelled molecules to proteins, enzymes as well as nanoparticles that helps to determine the amount of labelled proteins that is entrapped in the capsules and well as in walls of the capsules. This is one of the most common techniques used to understand the loading process in capsules fabricated using Layer-by-Layer tool. This instrument was also used for characterizing the protein expression detection for DNA delivery projects.

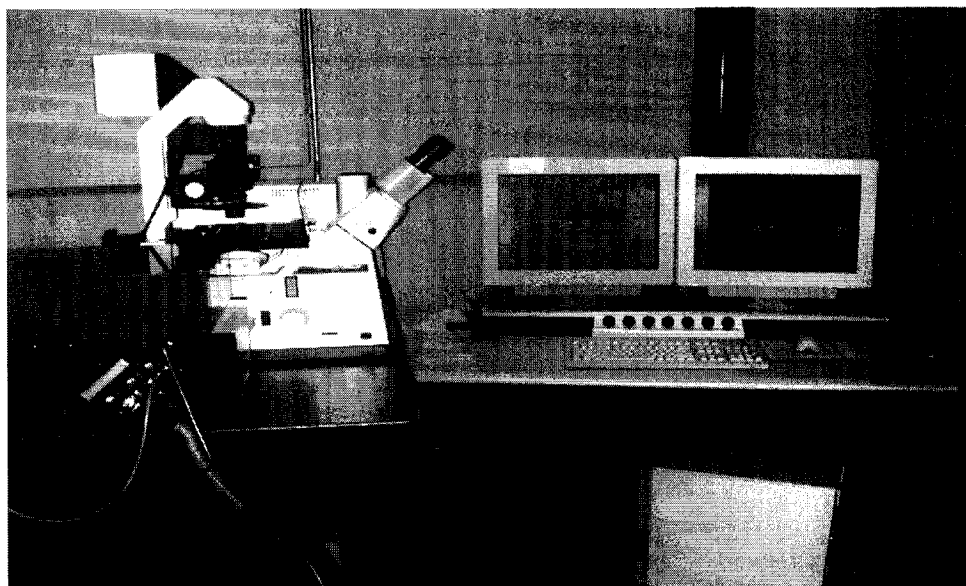


Figure 3.5: Picture of Confocal Laser Scanning Microscope Instrument

3.6 UV-vis Spectroscopy

Many compounds absorb ultraviolet (UV) or visible (Vis) light. When a beam of light of a particular wavelength is passed through the solution absorption occurs. Thus if all the light passes through a solution without any absorption, then absorbance is zero, and the percent transmittance is 100%. If all the light is absorbed then percent transmittance is zero. This absorption is given by Beer-Lambert Law:

$$\mathbf{A = ebc}$$

Where **A** is absorbance

e is molar absorptivity with units of $L/mol \cdot cm$

b is path length of the sample in cm, that is the path length of cuvette in which sample is contained

c is the concentration of the compound in solution and is given by mol/L

Hence, absorbance is proportional to the concentration of the solution. Thus UV-Vis spectroscopy is used as one of the characterization of the LbL film on the quartz slide.

Therefore, as the films are developing, the absorption goes on increasing, which is an indication of film growth. This instrument was also employed for assay characterization.

CHAPTER 4

PROTEIN ENCAPSULATION IN THIN WALL POLYION MICROSHELLS

4.1 Introduction

A thinfilm assembly by means of alternate adsorption of oppositely charged linear polyions was introduced in the mid-nineties by Decher et al [3]. The basis of this method involves resaturation of polyion adsorption, resulting in the reversal of the terminal surface charge of the film after deposition of each layer. The method provides the possibility of designing ultrathin multilayer films with a precision of one nanometer and with defined molecular composition. The assembly process elaborated for planar solid supports was adapted for microtemplates (colloidal particles with sizes of 0.2 to 5 microns, e.g. latex spheres, microcrystals, biological cells and other colloids) [61, 62, 66, 68, 74-83]. In this process, a linear polycation solution is added to the suspension of colloid particles, and after adsorption saturation, particles are separated from free polycations in solution. Then, a linear polyanion layer is deposited (Fig. 4.1). In the same manner, one can deposit any number of polyion layers on the core. A typical polycation / polyanion bilayer thickness in such a process is 4-5 nm [68]. After the shells are formed,

one can dissolve the core particles to obtain empty capsules with a wall thickness tuned in range from 10 to 50 nm and with needed composition [61, 62, 66, 68, 75-77]. A shell material and layer number can vary the permeability properties of polyion capsules. The wall permeability for macromolecules depends on pH: at low pH poly(styrenesulfonate)/poly(allylamine) capsule walls were opened, and at pH higher than 7.5 they were closed [68, 77-79] which probably is related to the pore formation due to misbalance of charges in the polycation / polyanion multilayer complex [70]. Molecules with weight less than ca 4,000 can penetrate through walls also in their closed state [77].

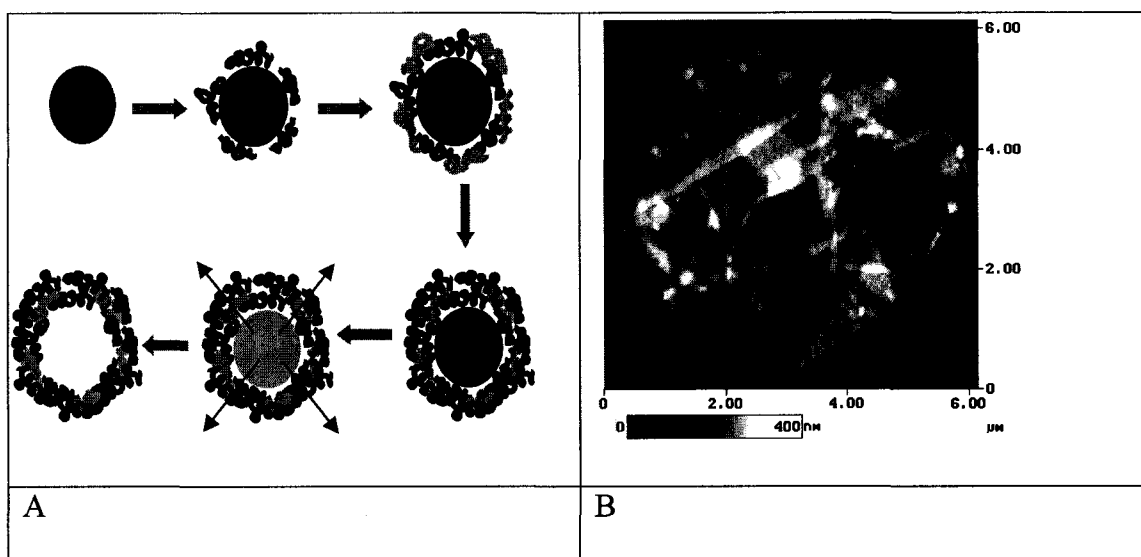


Figure 4.1: a-b Scheme of the capsule assembly and AFM image of dry 5- μm diameter (PSS/PAH)₄ capsule

By varying the pH of the capsule suspension in the presence of the proteins, one can open and close their wall pores and to perform an encapsulation. Therefore, one can encase enzymes inside the polyion capsules with nano-organized walls where they will be protected against high molecular weight inhibitors (such as proteases). Low molecular weight substrates (such as glucose) can easily penetrate inside the capsule by diffusion.

Construction of such enzymatic microreactors was recently demonstrated for urease, α -chymotrypsin and peroxidase [79, 80].

In this work, as a part of our efforts to create a new protein microcarrier, we demonstrate polyion capsule loading with glucose oxidase, hemoglobin and myoglobin and analyze some features of the loading process. In particular, a concentration of proteins inside the capsules, a ratio between the mass of the encapsulated proteins and the mass of the polymer shell, the mass of proteins which are bound to polycation/polyanion walls, and an enzymatic activity of encased glucose oxidase were studied.

4.2 Experimental Procedure

4.2.1 Microencapsulation

We encapsulated proteins in microshells assembled via layer-by-layer assembly of linear polycations and polyanions on a 5- μ m diameter template. Hollow polyelectrolyte capsules were fabricated at pH 6.5, 0.5 NaCl by alternate adsorption of four bilayers of sodium poly(styrenesulfonate) (PSS) (Aldrich, MW 70,000) / poly(allylamine) hydrochloride (PAH) (Aldrich, MW 50,000), onto 5- μ m diameter melamine formaldehyde (MF) particles (Microparticles GmbH, Berlin). For the multilayer shell formation, $\sim 10^{11}$ core particles were added to a 2-mL Eppendorf centrifuge tube followed by the addition of polyions to give shell architectures of the following sequence: (PSS/PAH)₄₋₆. After addition of the polyions, 15 min were allowed to elapse so that saturation adsorption of the polyions on the colloid particles was reached. The coated latex spheres were then centrifuged at 300 g, and the supernatant containing the unadsorbed species were removed. This procedure was repeated three times after the

adsorption step to avoid admixing of the sequentially deposited components. To dissolve melamine formaldehyde cores, we decreased pH to 1.

The capsules prepared via alternating adsorption of oppositely charged poly(allylamine hydrochloride) and poly(styrenesulfonate) with composition (PSS/PAH)₄₋₆ have been shown to be permeable to macromolecules at pH values below 6 and closed at pH above 7.5 (Fig. 4.2).

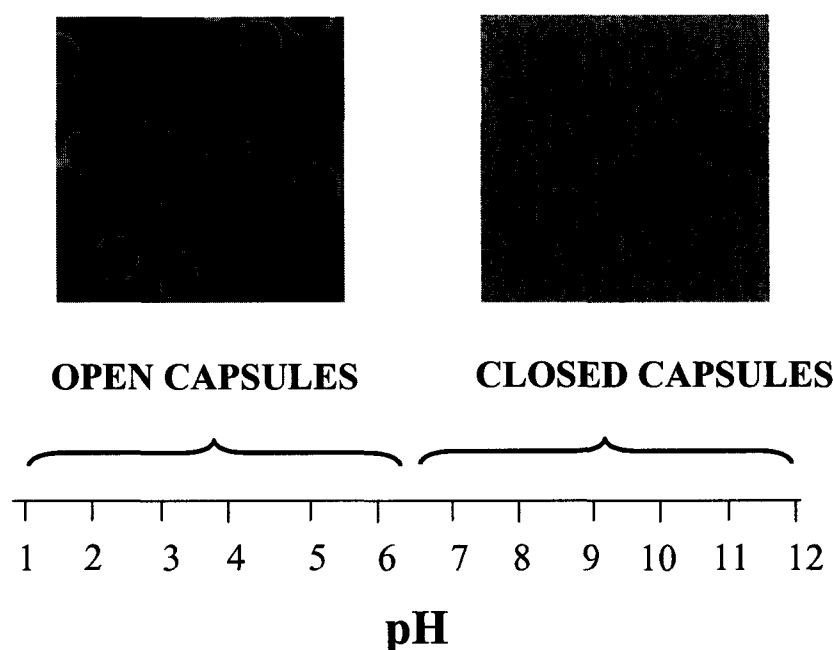


Figure 4.2: Confocal cross-sectional images of (PSS/PAH)₄ capsules with open wall pores (at low pH) and closed pores (at high pH). FITC labeled dextran (MW 70,000) was added to the solvent as fluorescent indicator

For loading, 0.2 mL of capsules and 0.2 ml of proteins with concentration 2 mg/ml were incubated at pH 6 for 20 min. Then the pH of solution was adjusted to pH 10 and remaining proteins were washed out three times with 2 mL water and centrifugation, so that final pH = 8.

Glucose oxidase, bovine hemoglobin and myoglobin (all from Sigma) were used without further purification. These proteins were labeled with fluorescein isothiocyanate (FITC)

(Sigma) by incubation with the marker (mass ratio protein / FITC was 30/1) in pH 9 boric buffer for 3 hours at room temperature and further purification with chromatography on G-50 Sephadex (Sigma) as a carrier following a procedure described in [79].

4.3 Instruments

The Confocal microscope Leica TCS SP, equipped with a 100x/1.4-0.7 oil immersion objective was used for visualization of the microshell cross-sections. The investigated capsule suspension was placed between a glass slide and a cover slip glued at the edges. Excitation wavelength 488 nm was chosen according to fluorescein labels. The fluorescence intensities of the scanned capsules were measured and processed with Leica TCS software. The scanning force microscope Nanoscope III Multimode SFM (Digital Instrument Inc., Santa Barbara, CA) was used in tapping mode and images were processed with Nanoscope software. Samples were prepared by applying a drop of capsule suspension onto a freshly cleaved mica support. Eppendorf centrifuge was used for a capsule preparation. UV-vis spectra measurements were performed on HP-Agilent 8453 spectrophotometer (USA).

4.4 Glucose Oxidase Activity Assay

To measure the activity of the glucose oxidase (GOx) multilayers, we used an assay recommended by Sigma: 2.4 mL of 0.21 mM o-Dianisidine solution in 50 mM sodium acetate buffer (pH 5.1), 0.5 mL of 10 % (w/v) β -d-glucose solution and 0.1 mL of a peroxidase solution (containing 60 units mL⁻¹) were mixed in a cuvette and air-equilibrated until the absorbance at 500 nm was constant. GOx or capsules were added, and absorbance data were recorded continuously for 4 min, starting immediately after

mixing. For each experiment, the same enzyme concentration was added to this test solution. The assay is based on production of H_2O_2 in the enzyme-substrate reaction; the peroxide is in turn consumed by peroxidase to result in catalytic oxidation of dianisidine, resulting in dark red coloration (maximum absorbance at 500 nm).

4.5 Results and Discussion

4.5.1 Glucose Oxidase and Hemoglobin Encapsulation

Figure 4.3-4.4 shows confocal and AFM images of 5- μ m diameter (PSS/PAH)₄ capsules loaded with FITC labeled hemoglobin and GOx. In both confocal pictures, capsule cross-sectional images indicate the presence of the labeled protein inside the capsules and the absence of labeled proteins outside. The walls of the capsules are brighter than the interior, showing that the larger density of labeled proteins is in the polyion walls. Next to the images we presented brightness curves indicating the amount of the protein inside and outside of the capsule. Figure 3b shows a typical AFM image of the dried loaded capsules. One can see that during drying, the capsule collapsed and some material from inside was seen next to the defective part of the capsule.

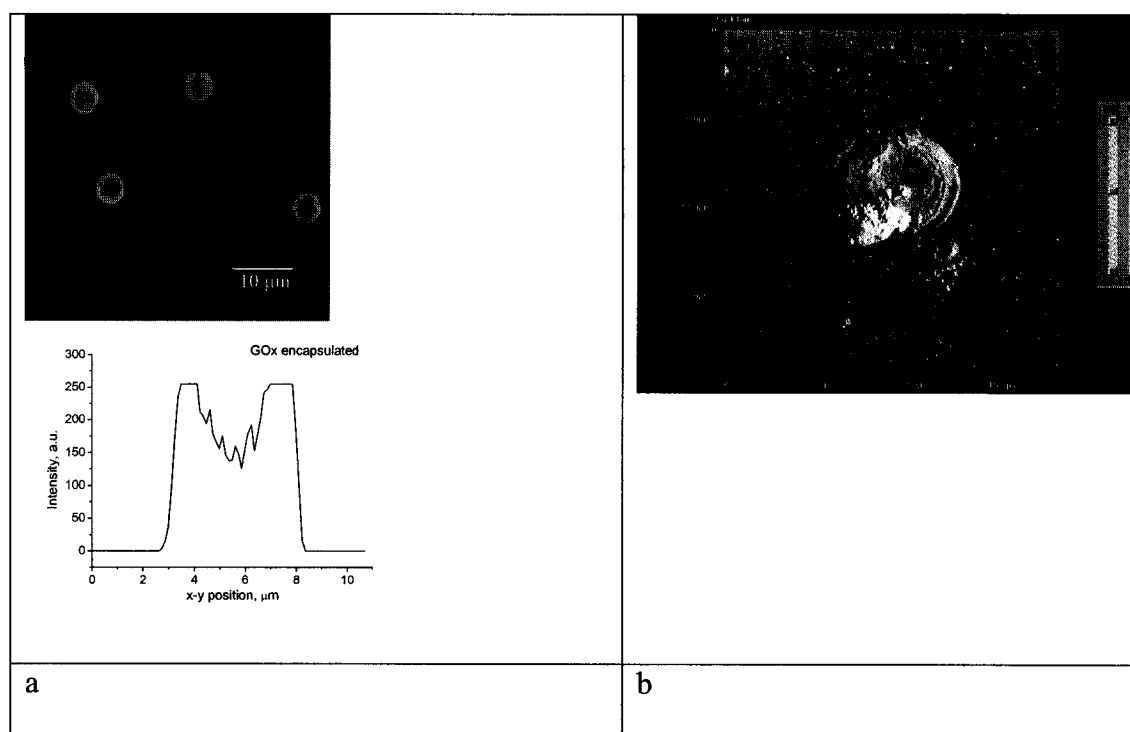


Figure 4.3: FITC-GOx loaded capsules: a- confocal cross-sectional image in solution at pH 8 and the fluorescent intensity profile. b – AFM tipping mode image of the dry broken capsule on mica surface

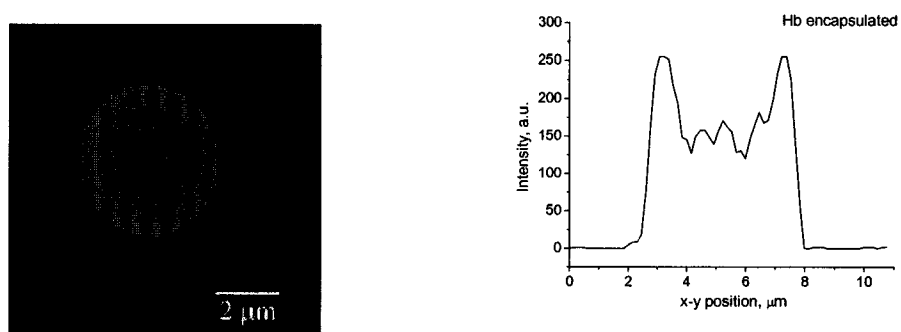


Figure 4.4: FITC-hemoglobin loaded capsule: Confocal cross-sectional image and fluorescent intensity profile of the capsule

Let us estimate the capsule dimensions: for 2.5- μm radius and 20-nm thick (PSS/PAH)₄ shell [76] we have a total capsule volume of $V_c = 65 \cdot 10^{-12} \text{ cm}^3$, while the volume of the polyion shell only: $V_s = 9.4 \cdot 10^{-13} \text{ cm}^3$. Taking hydrated polyion density as ca 1.05 g/cm³, one has the shell mass of $M_s = 9.8 \cdot 10^{-13} \text{ g}$.

How much proteins are encased into the capsule? For loading, we mixed an equal amount of the shell dispersion and 2 mg/mL protein solution. Concentration of loaded capsules was calculated by a direct count of dried capsules suspension done from the optical microscopy; for myoglobin loaded capsules it was $N = 10.5 \cdot 10^6 \text{ cm}^{-3}$, for hemoglobin capsules it was $N = 8.5 \cdot 10^6 \text{ cm}^{-3}$, and for glucose oxidase $n = 3 \cdot 10^6 \text{ cm}^{-3}$.

Concentration of proteins in the capsules was determined with Loury method [84] and was found $C = 0.02 \text{ mg/mL}$ for myoglobin and hemoglobin and $C = 0.007 \text{ mg/mL}$ for GOx. Dividing these values on the number of capsules in one milliliter, one obtains the protein loading in one capsule $M_{Mb} = 0.19 \cdot 10^{-11} \text{ g}$, $M_{Hb} = 0.24 \cdot 10^{-11} \text{ g}$, $M_{GOx} = 0.23 \cdot 10^{-11} \text{ g}$. The concentrations of proteins in the capsules will be $C_{Mb} = 29 \text{ mg/mL}$, $C_{Hb} = 36 \text{ mg/mL}$, and $C_{GOx} = 35 \text{ mg/mL}$,

Comparing this weight with the weight of empty dry shell ($9.8 \cdot 10^{-13} \text{ g}$), one finds that shell mass consists of 30 % of the dry mass of loaded capsule and proteins give ca 70 % of the loaded capsules mass.

It is remarkable that concentration of loaded proteins (29-36 mg/mL) is higher than concentration in protein solutions used for the loading (ca 1 mg/mL). Probably, some unclear mechanism exists which “pumps-in” proteins inside the shells.

4.5.2 Hypothesis:

- The shell wall have negative charge at the inner surface (first layer was poly(styrenesulfonate)) and positive outermost layer (poly(allylamine). This asymmetric wall can provide a driving force for increased protein concentration inside the capsule as compared with concentration at the loading solution.
- Another reason may be in protein/polyion complex formation in the capsule multilayer wall. Later, we have shown with Myoglobin loading that this mechanism could be responsible for ca 20 % from the total loaded proteins.
- It was earlier reported that while using MF as a template for fabrication of hollow capsules there are some MF oligomer remaining in the capsules. This oligomer is positively charged and hence during the loading of proteins they form complexes and higher concentration of proteins is seen inside the capsules.
- When Ficks law of diffusion is applied to molecular diffusion across charged membrane, one can draw an analog stating that the rate of diffusion of molecules across charged capsule walls is directly proportional to the potential barrier across the wall and inversely proportional to the thickness of the capsule wall. The potential barrier across walls fabricated for 4 bilayers of PSS/PAH is +10 mV which means that it aids in the entry of proteins inside the capsules. In addition MF(oligomer)/PSS complex which has a high +ve charge along with +ve potential barrier creates electrostatic force which attracts proteins inside the capsule but also slows down or completely hinders the diffusion of proteins out of the capsules.

Proteins encased in the capsules preserved their bioactivity as it was shown earlier for urease, α -chymotrypsin and peroxidase [79, 80], and it will be demonstrated below for glucose oxidase. GOx loaded in capsules, initially shows 60 % of activity as compared with the enzyme solution, and it dropped to 35 % after 15 days, to 10 % after 70 days, and to 6 % after 85 days after encapsulation (capsules were kept at 25° C first two days and then at 5° C) (Fig. 4.5). All activity checks were performed with FITC-labeled GOx.

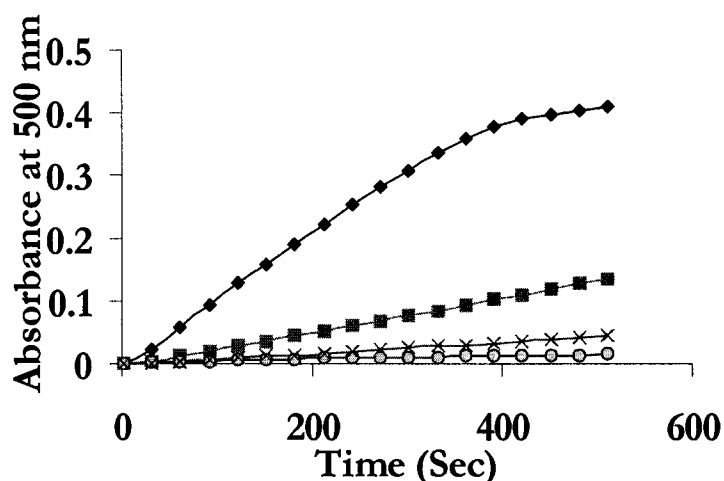


Figure 4.5: FITC-GOx bioactivity (proportional to the absorbance increment) for the equal enzyme amount (0.007 mg/mL) free in solution (diamonds) and in the shells 15 days after encapsulation (squares), 70 and 85 days after encapsulation (red and blue)

It is of interest to compare our data with glucose oxidase bioactivity in solution and assembled in the polyion films [85]. GOx enzymatic activity in the film assembled by alternation with polycation was 80 % as compared with the enzyme solution, and it dropped to 22 % after 28 days keeping at 25 C. These results are close to our results, but in the capsule GOx activity produced by the enzymes bound to the walls and the enzymes

encased inside the capsules, and the storage properties of the GOx in these two states may be different.

One of the purposes of this study was to conduct encapsulation in a way that does not affect the native structure of proteins. It is important for enzymes to keep their activity and for hemoglobin to maintain its oxygen-binding ability. It was established [86] that the spectrum of hemoglobin is very sensitive to the changes of hem conformation and the maximum adsorption at 409 nm (Soret band) shifts by more than 2 nm if any changes occur. The spectrum of capsules with FITC-labeled hemoglobin encapsulated (Fig. 4.6) was recorded for verification of possible changes that could occur during loading or due to the contact of the protein with the capsule wall. No shift of Soret band was registered; only the second peak corresponding to the fluorescein marker appeared at 496 nm. Therefore, hemoglobin in the capsules preserved its native conformation. Though hemoglobin was encapsulated in the capsules there was no observation of scattering in the spectrum because the polymers have absorbance below 300nm and the spectra collected is above 300nm.

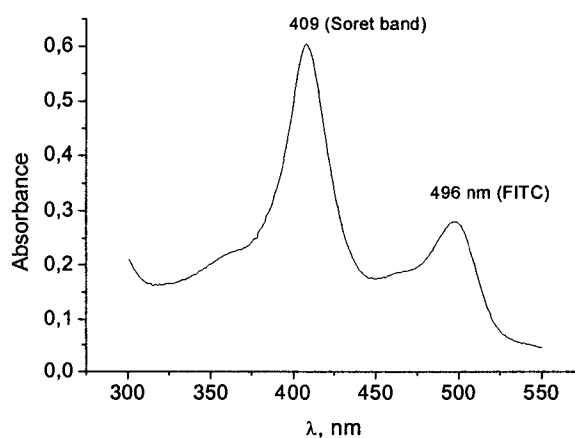


Figure 4.6: UV-spectrum of encapsulated FITC-hemoglobin, pH 7.5

4.5.3 Myoglobin Encapsulation

Myoglobin encapsulation was performed in a similar manner into (PSS/PAH)₄ capsules (Fig. 4.7), and loading of $(0.19 \pm 0.05) 10^{-11}$ g per capsule was found. This loading is less than loading of glucose oxidase and hemoglobin in spite the initial concentrations of these proteins used for the loading were similar. Probably, a smaller molecular weight and dimensions of myoglobin (as compared with hemoglobin and GOx, correspondingly, 17,800; 64,000 and 186,000) result in its partial leakage from the capsules.

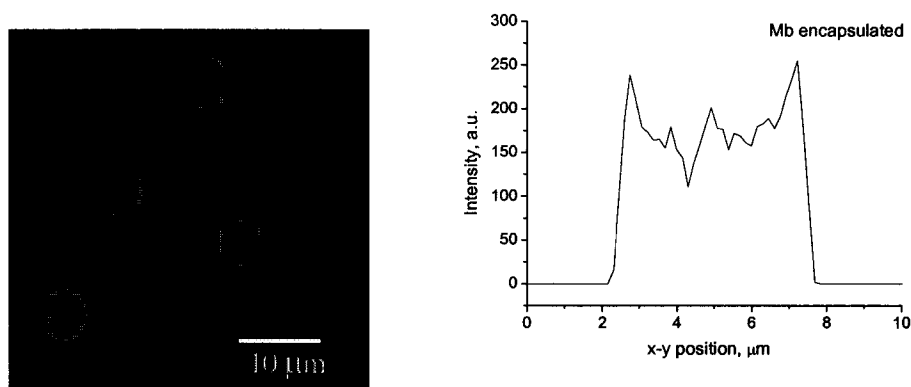


Figure 4.7: Confocal cross-sectional image of FITC-Mb loaded capsules and fluorescent intensity profile of the capsule

Above, we gave a total amount of myoglobin encased inside the capsule. Further we will estimate an amount of the protein bound to the capsule walls only. For this we prepared the capsules with open (broken) walls (i.e., capsules unable to keep Mb inside, as it was evident from confocal images of labeled Mb admixed with the empty shells). Figure. 4.8 shows these two routs of the myoglobin encapsulation.

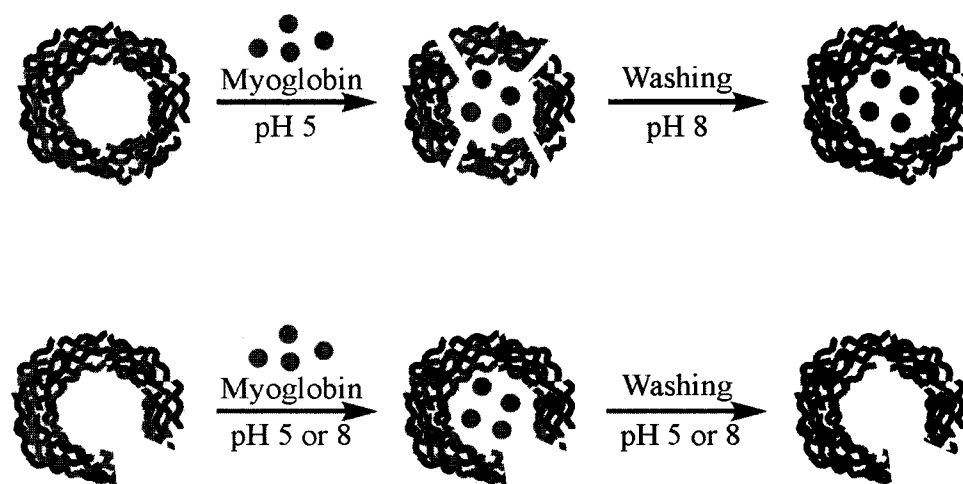


Figure 4.8: Scheme of the two routes of myoglobin encapsulations based on pH variation for unbroken (upper route) and broken (lower route) shells

4.5.4 Myoglobin Complexation with Open (Broken) Shells

Turning attention to discuss myoglobin loading to the walls of the open (broken) shells, these shells were obtained by PSS/PAH assembly on the special MF cores with higher degree of polymerization. Such cores, during dissolution at low pH, broke the capsule walls that could be proved by CLSM experiments with FITC-labeled myoglobin.

Loading was performed by adding myoglobin to the capsule dispersion. The protein concentration was 0.7, 1.4, 3.4 and 6.8 mg/mL. Loading was performed both at pH 5 and pH 8 to broken capsules (with washing after the loading). The resulting concentration of myoglobin bound to the shells was determined from Soret band maximum (409 nm, hem absorbance) at pH 8 when capsules were washed out from myoglobin solution.

Table 4.1 and Figure. 4.9 show that the mass of myoglobin bound to one broken capsule depends on the shell's outermost charge and initial protein concentration. We found that binding at pH 5 was more effective than at pH 8. Besides, at pH 5, Mb binding to broken capsules with anionic (PSS) outermost was twice as efficient as for using the capsules

with cationic (PAH) exteriors. The isoelectric point of myoglobin is at pKa 6.8, and at pH 5 myoglobin has charge +10 [58]. This phenomenon could explain larger myoglobin adsorption in capsules with anionic outermost layers. Myoglobin constituted ca 50 % of the mass of the capsule with (PSS/PAH)₅+PSS wall immersed into more than 3 mg/mL of myoglobin solution (Table 4.1).

Table 4.1: Myoglobin loading in (PSS/PAH)₅ + PSS broken shells, pH 5 (with washing after loading at pH 8)

Protein concentration mg/mL	Protein per one capsule $\times 10^{-12}$ g	Mb part from total mass of capsule wall
0.7	.33	25 %
1.4	.43	31 %
3.4	.96	49 %
6.8	1.06	52 %

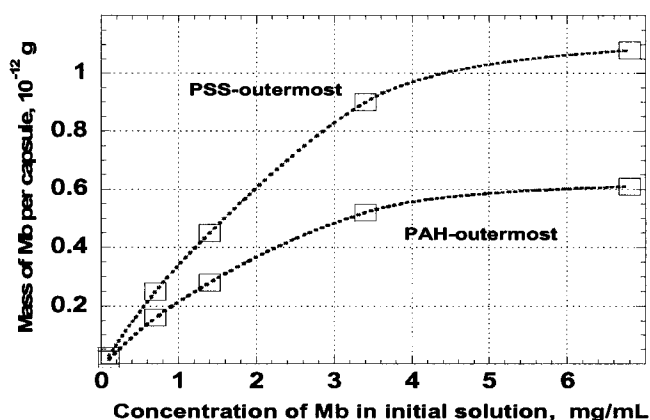


Figure 4.9: Loading of myoglobin in the shell wall depending on the protein concentration in the initial solution and on the outermost of the capsules, loading at pH 5, washing at pH 8

Let us analyze an amount of encased and bound myoglobin for initial loading concentration of 1 mg/mL. An amount of myoglobin bound to the capsule walls is $0.38 \cdot 10^{-12}$ g as established from its adsorption to broken capsules, which is ca 20 % of Mb encased in intact unbroken shells ($0.19 \cdot 10^{-11}$ g per capsule).

An Atomic Force Microscopy (AFM) analysis of the loaded shells has shown regularly distributed mottled appearance with average diameter of (50 ± 20) nm (Figure. 4.10). These “blisters” were not found on empty unloaded shells. We assume they could be stoichiometric complexes formed by cationic myoglobin and anionic PSS. We have to mention that the capsule wall assembly was performed from polyion solutions in 0.5 M NaCl; therefore, not all ionized groups of PSS and PAH “locked” one with another, and remaining charged groups can react with oppositely charged regions on the Mb globule surface. Formation of similar 100-nm diameter complexes for albumin/polycations coacervates was found by Kabanov [87]. This new formation is an indication of Mb bound on the capsule walls. A diameter of the “blisters” is close to the capsule wall thickness (30 nm for six bilayers), which indicates that they penetrate the walls. There are ca 230 “blisters” per $1 \mu\text{m}^2$ and they occupy ca 40 % of the capsule surface showing two-dimensional close-packed picture. The capsule surface is $78.5 \mu\text{m}^2$, therefore, we have ca 18,000 “blisters” per capsule. Such blisters were never detected for (PSS/PAH)-capsules, but they are rather similar to “grains” of (90 ± 10) nm diameter found for (PSS / poly(dimethyldiallyl ammonium chloride))₅ capsules [88]. Authors of [88] also proposed that the grains are specific complexes of several polyion molecules.

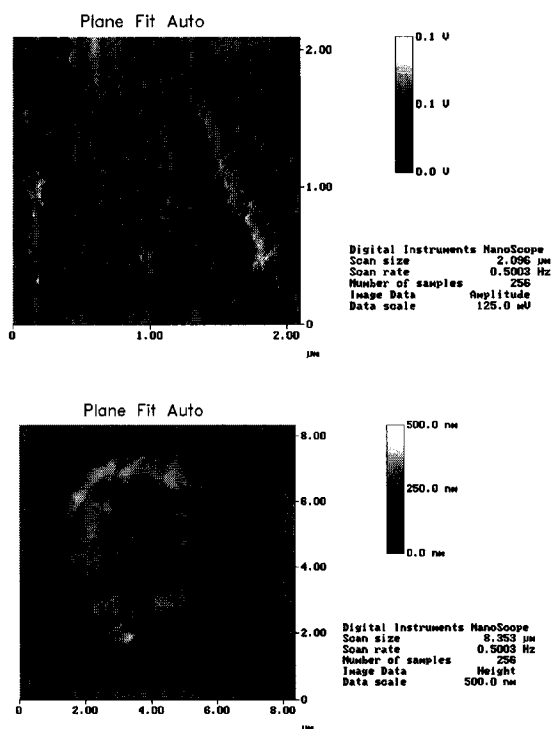


Figure 4.10: AFM capsule image of open-wall capsule with 3 mg/mL myoglobin loading concentration. (Image taken at Max Plank Institute in collaboration with Dr Dmitry Schukin)

4.6 Conclusions

We presented results on loading myoglobin, hemoglobin and glucose oxidase into polyion microcapsules. Earlier, it was reported about loading to the similar capsules of α -chymotrypsin (MW 25,000) and urease (MW 34,000) [11-12]. Analyzing the process of loading these proteins to the (PSS/PAH)₄₋₆ polyion capsules, we can conclude:

By opening capsule pores at low pH and closing them at high pH, one can load inside proteins with concentrations much higher than the concentration of the initial protein solution. At the concentration of loading proteins of 1 mg/mL, they result in ca 30 mg/mL protein concentration in the globules and proteins consist 70 % of total mass of the globule, and mass of the polymer shell is 30 %. The loading features were similar for

these proteins with mass range from 17,800 to 186,000. Biological activity of glucose oxidase was 60 % as compared with the activity of free enzyme in solution, and dropped to 20 % of the initial activity after two months storage at 5° C.

Additionally to the proteins encased inside the capsules, there are proteins bound to the capsule walls. For myoglobin, the amount of such bound proteins increases with concentration of myoglobin in solution used for the loading and reached a saturation at $C = 3.5 \text{ mg/mL}$. The mass of this largest amount of myoglobin bound to the capsule wall approximately equals to the half of capsule mass. Therefore, we have the following approximate composition for 5- μm diameter (PSS/PAH)₄ shell loaded with 1 mg/mL myoglobin solution: 55 wt % of the mass are encased proteins + 15 wt % bound proteins + 30 wt % the shell mass, and total concentration of myoglobin in the capsule is 29 mg/mL. This is only a general estimation and it can be changed with varying a concentration of the proteins used for the encapsulation.

CHAPTER 5

NANOPARTICLES FOR DNA DELIVERY USING

LBL TECHNIQUE

Transfecting foreign DNA into cell culture and *in vivo* is under consideration. Layer-by-layer constructed nanoparticles were designed for safe and targeted delivery of foreign genes. The nanoparticles were constructed using a 78 nm silica core particle, on which deposition of DNA, poly (ethyleneimine), and target assisting molecules were assembled in nano-organized manner. The targeting moieties included N-acetyl-d-galactosamine, poly(arginine), Protamine, and lipids. The targeted cell type is hepatocyte, they have asialoglycoprotein receptors on outer surface. These receptors contain the carbohydrate recognition domains that can endocytose large particles when bound and have also shown affinity towards galactosyl residues. By coating the outer layer with lipid, the nanoparticle can enter the cell through permeating the cell membrane. We found the size of nanoparticles is more critical for lipid coated than for sugar coated particles when delivered to liver cells. Nanoparticles ranging up to 300 nm are permeable to liver derived cells. We report the development of a layer-by-layer method for creating nanoparticle based gene delivery vectors. The layer-by-layer nature of particle construction allows greater flexibility and fine control of not only

what is delivered to the cell, but also it can be designed in the later stages eventually, how these components are released into the cell.

5.1 Introduction

Layer-by-Layer (LbL) self-assembly technique has spread its applications in various aspects of sciences since its adaptation. This technique has come forward since its early applications in nineties with its simplicity of polyion adsorption. [3, 6, 21, 29]. With the span of time since its implication this alternate adsorption can be used for several species such as charged polymers, proteins, lipid bilayer, biospecific complexes, bola-ampiphiles, conductive polymers and organic dyes [89-93] Thin films obtained are in the range of few to hundreds of nanometer with a precision of one nanometer and in a nanoorganized manner. With its varied choice of biocompatible materials the microshells have found its application in various medical fields among which study of drug release properties, delivering loads to specific sites and forming biosensor are most common. [94-96]

Various approaches are emerging towards gene therapy. The basic gene therapy should have:

- Gene delivery system,
- A gene that encodes the proteins
- The plasmid that controls the functioning of the gene within the cell [97].

Biodegradable polymers have been used from drug delivery to tissue engineering and have even advanced to the gene therapy, which allows us its use for LbL construction of nanoparticles to attain a vector component for gene expression. [98,99] The most common and also effective method for gene delivery is to form complexes with DNA

using poly(ethyleneimine) [100,101], poly(lysine) [100, 102], chitosin [100], lipids and many other biodegradable polymers [103] which can achieve gene medicine. Some other approaches involves naked DNA, “gene gun”, chaser injection and electroporation [100, 101].

Existing gene delivery systems have a variety of limitations:

- These systems are designed to eliminate an infection by transferring a therapeutic gene to host cells, however, they have been largely unsuccessful since only low doses of genetic material can reach the target specific cell types that are infected
- Increased side effects are also due to non specific targeting of non infected cells with genes
- Host cells reaction to the carrier molecules used associated with their gene delivery

As such there is currently a need for a gene delivery system that has minimal side effects but high potency and efficiency. One such system could be that of the Layer-by-Layer self assembled nanoparticles coated with targeting biomolecules. A novel concept of LbL also allows modifying the polymer surface by electrostatically attaching specific targeting molecules that can be organized with precisions of nanometer for gene expression. A specific cell line can be targeted with this vector in a cell population. Thus, nonviral gene delivery systems can be designed with idealized structural and chemical properties that can enter through the receptor in the cells. The receptor on the targeted cell asialoglycoprotein (ASGP) receptor has reported to show high affinity for galactosyl residue. In our approach to achieve transfection we chose

targeting moieties such as N-acetyl-d-galactosamine (gala), [104] poly-l-arginine (parg) [105] and protamine sulphate [106,107] as the outer coating of the nanoparticle vector. The targeting moieties on the polymer have been used as promoters for delivery and gene expression. [104-107]. Bionanoparticle complexes, while still in their infancy as a new bionanotechnology, hold great promise for more sophisticated targeting and controlling drug/gene delivery to specific cells. Delivery of the drug/gene to a cell surface by conventional targeting does not insure that it is delivered to the site of required action within the cell. The nanosystems can contain intracellular targeting molecules that re-direct the nanomedicinal system to the correct intracellular location for specific molecular and biochemical actions. For example, the interior of a 10-micron diameter cell is much higher than the volume of an individual 100 nm diameter nanoparticle. Prior studies using confocal microscopy have been used to verify that the drug/gene is targeted to the correct location within the single cells.

5.2 Ideology/Strategy



Figure 5.1: Targeting nanoparticle Ideology/Strategy

The strategy for the gene delivery and gene expression is on the basis of endocytosis of the nanoparticles through the asialoglycoprotein receptor on the Huh-7 cell lines and disassembling of nanoparticles within the cells. Targeting this receptor for the entry to the cells would be possible by different outer layer moieties that can have affinity towards the receptors. LbL method allows architecture design of nanoparticles with needed configuration of different species in the shells. The mechanism can be idealized for the nanoparticles if they were taken up by the receptor rather than just penetrating in the cell lines. Lipid-coated particles have reported to work with mechanism as well as without mechanism. As the nanoparticles are uptaken by the cells, the cell wall forms a membrane bound vesicle around the targeting vector. Following the endocytosis of the nanoparticles the pH drops about 3 to 4 in the membrane bound vesicle, this helps the layer by layer assembled nanoparticles to take advantage of the environment to disassemble thus leaving the plasmid DNA free. For gene expression the synthesis of RNA by RNA polymerases using a DNA template (transcription) should take place where further RNA translates to the protein expression. For gene therapy the sequence of events occurring in line would be the task of our targeting nanoparticle. Complex multilayered nanoparticles hold great promise for more sophisticated drug/gene delivery systems to single cells. Outermost layers can include cell targeting and cell-entry facilitating molecules. The next layer can include intracellular targeting molecules for precise delivery of the nanoparticle complex inside the cell of interest. Importantly the full nanoparticle system can be used to prevent any cells from encountering the drug unless that cell is specifically targeted.

5.3 Materials and Methods

5.3.1 Materials

The 78 nm Silica particles used as cores were obtained from Nissan Snowtex. The inner layer of PEI (mol. Wt 10000 gm/mole) was purchased from Polyscience. The plasmid DNA was produced at UTMB, Galveston, Texas. The outer targeting moieties N-acetyl-d-galactosamine (GALA) (221.2 gm/mole), poly-l-arginine (14000 gm/mole) and protamine sulphate (5120 gm/mole) and Lipofectamine 2000 (lipid) were products of Sigma. The media used for preparation of the nanoparticles were 20 mM Tris buffer and .5M NaCl salt also products of Sigma. The cells were stained with DAPI (blue, Molecular Probes, Inc.) and for cell culture and transfection FBS and Penicillin/Streptomycin were also purchased from Sigma.

5.3.2 Fabrication of Nanoparticles by LbL

100 μ l of 78 nm silica particle solution was taken and 400 μ l of PEI (mol. Wt 10,000 gm/mole) at 2mg/ml concentration was added to it, and the mixture was allowed to self assemble for 15 min. Layer-by-Layer deposition of oppositely charged polyelectrolyte on the core was observed. **[Figure 5.2: Schematic of LbL particles]** The mixture was centrifuged at 7000 rpm for 8 min and supernatant was removed. Three washes were given after each deposition of layer. Following the PEI layer, plasmid enhanced green fluorescent protein (DNA) was deposited. Depending on the charge of the outer targeting layer N-acetyl-d-galactosamine and lipid monolayer were deposited on DNA. The layer deposition and washing process was continued till the nanoparticles of desired composition were obtained.

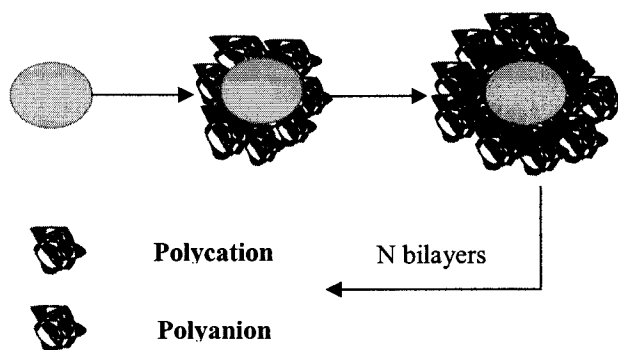


Figure 5.2: Schematic of LbL

5.3.3 ζ Potential Measurements and Particle Sizing

Deposition of oppositely charged layers was characterized with the help of ζ Potential measurements [Figure 5.3: Charge measurement of LbL assembly through Zeta].

The measurement of the sizing of the LbL fabricated nanoparticle was performed by Particle sizing. These measurements were carried out in Zeta Plus Particle Analyzer (Brookhaven Instruments Corp., Holtsville, New York)

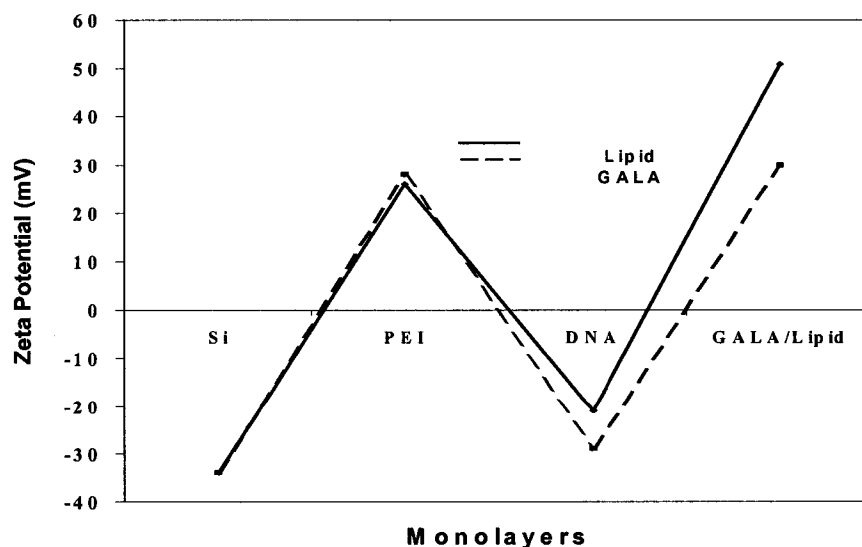


Figure 5.3: Charge measurement of LbL assembly through Zeta

5.3.4 Quartz Crystal Microbalance

The thickness of the layers in LbL can be organized precisely and in the nanometer range. This characterization is done with the help of Quartz Crystal Microbalance (Sanwa Tsusho Co., Ltd., Japan). The resonator is used as the depositing surface and after each deposition of the layer the frequency shift is noted. The frequency shift is proportional to the thickness of layer deposited. Here the deposition of the different layers is characterized. [Figure 5.4: QCM Characterization of LbL assembly]

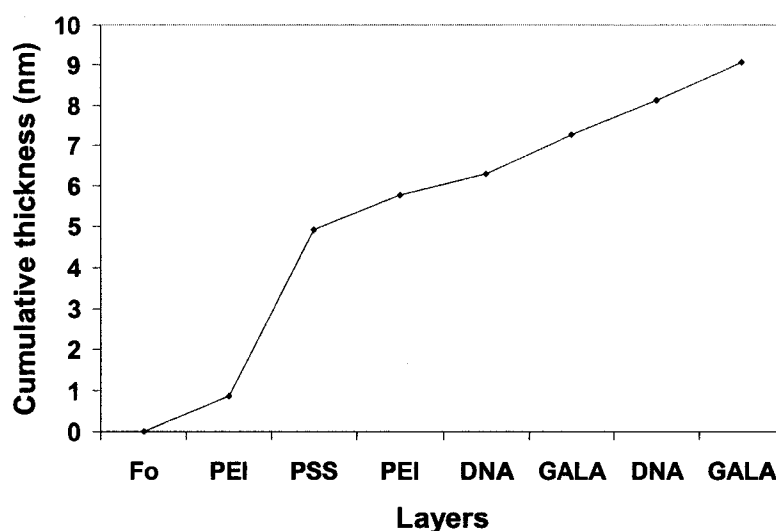


Figure 5.4: QCM Characterization of LbL assembly

5.3.5 Atomic Force Microscopy Characterization

The nanoparticles assembled through the LbL have different sizes ranging from 126 nm, 210 nm, and 1500 nm. The nanoparticles are constructed from depositing PEI (10000 gm/mole) layers on silica particles. The diameter of the PEI is .2 nm and the length of the polymer is 51 nm approximately. The alternate layer deposited was DNA of diameter 2nm and length of 2526 nm approximately. The length of the DNA molecule are too long, so during the process of the assembly several silica particles in

the solution attaches to the DNA, thereby increasing the size. Two more monolayers of PEI on the DNA and thereafter DNA on PEI were deposited, thus increasing the size of the nanoparticle. Before addition of the final targeting moieties, the DNA forms complexes with PEI and condenses on the nanoparticles. Thus, the particles of higher size ranges are produced. Also, the sample preparation was done in different media. The nanoparticles with size ranging from 126 nanometer were prepared in DI water, the 210 nm size nanoparticles were prepared using 20mM of Tris buffer and .5M NaCl salt whereas the 1500 nm size nanoparticles were prepared with only 20 mM Tris buffer. Figure 5.5 shows smaller particles of 100-nm size range, whereas Figure 5.6 depicts the size range of 200 nm. In Figure 5.7 it shows the aggregates of the particles and Figure 5.8 indicates different shapes and size of particles obtained. Atomic force microscopy images were obtained with a Q-Scope 350 AFM (Quesant Instrument corporation, USA) operating in tapping mode.

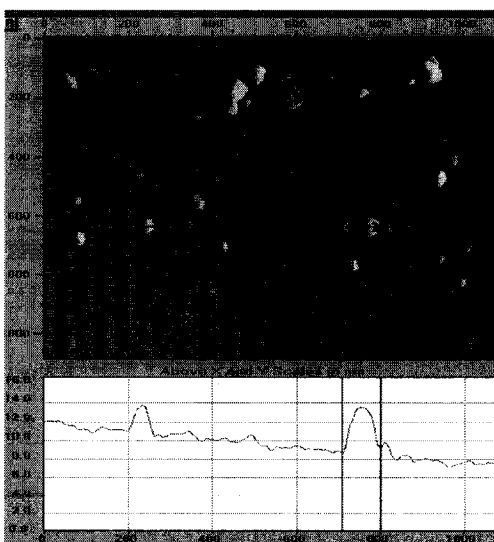


Figure 5.5: 100 nm size range nanoparticles characterized by AFM

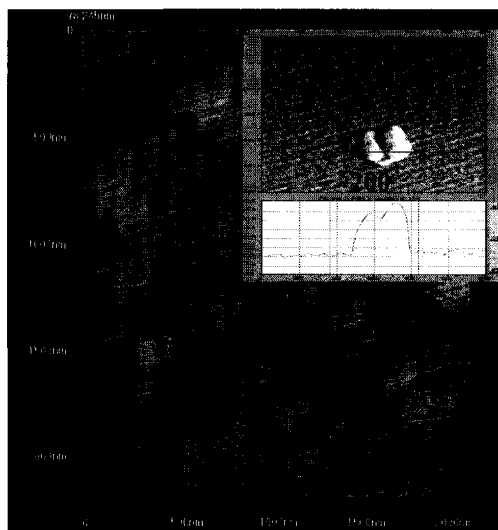


Figure 5.6: 300 nm range nanoparticles characterized by AFM

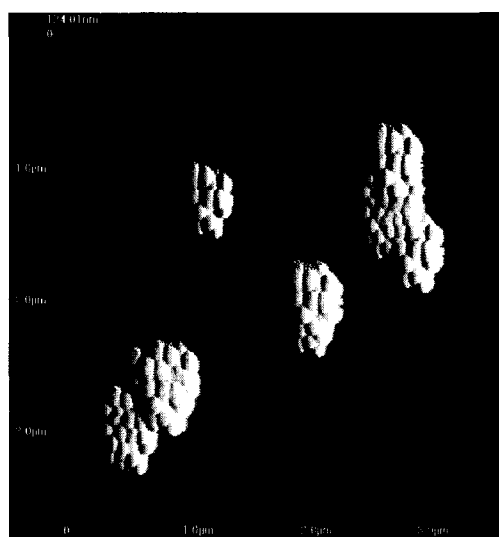


Figure 5.7: Agglomerates of several nanoparticles thereby increasing the size characterized by AFM

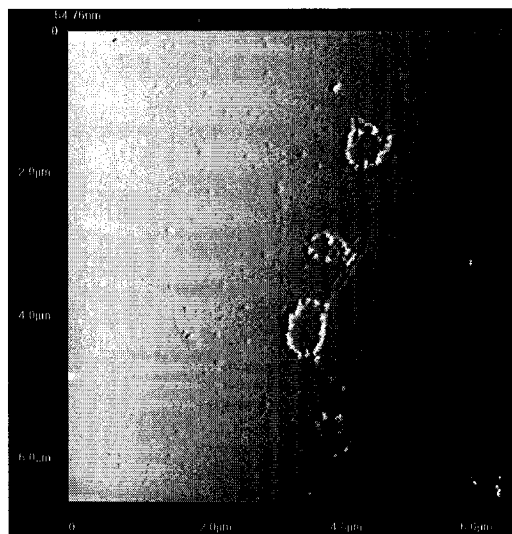


Figure 5.8: AFM picture indicating different shapes and size of nanoparticles

5.3.6 Cell Culture and Transfections

Cells were incubated at 37 C in 5% CO₂. Huh-7 cell lines were cultured in DMEM supplemented with 10% FBS and Penicillin/Streptomycin. Cells were transiently transfected with Lipofectamine2000 (Invitrogen, Inc.) using the manufactures instructions. Each experiment was done at least in triplicate and positive and negative controls were present in all experiments.

5.3.7 Confocal Microscopy

Cells were examined with a Zeiss 510 META confocal microscope. Excitation wavelengths depending on the fluorescent probes used. Appropriate emission wavelengths were determined and used for each fluorochrome used. Cells were analyzed with 20, 40, 63, or 100X objectives. A 20X objective was used for imaging large numbers of cells for analysis.

5.3.8 Flow Cytometry

Samples were analyzed by flow cytometry with either a FACScan (Beckton Dickinson, Inc.) or a home-built, high-speed cell sorter. Briefly, treated cells were trypsonized to attain a single cell suspension. Then, the cells were fixed, permeablized, and stained as described above. These cells were then filtered with a 70 μ m mesh cell strainer (Falcon) and analyzed by flow cytometry. GFP samples were excited using an Argon ion laser tuned to 488nm and detected after 488nm band reject and 530nm band pass optical filters (Omega Optical, Inc.).

5.4 Results

5.4.1 Effect of Size and Outer Coating on Cells

The nanoparticles were constructed using the surface charge chemistry of the components. The size of this vector can be controlled within the specific range this gives advantage in making the particles through this approach. Changing the core or the monolayer chemistry of the targeting moieties, the whole architecture of the nanoparticles can be designed. Several experiments were performed with one or more layers of DNA but it was concluded that one layer of DNA is efficient for transfection. LbL targeting nanoparticles were constructed and delivered to the cell. The nanoparticle had one of the layers as DNA and was constructed in size groups of 126, 210, and 1500nm all coated with GALA as targeting moiety. These nanoparticles were incubated with Huh-7 cells for 24 hours. After 24 hours the cells were counterstained with DAPI. The cells were then viewed, counted, and photographed with a confocal

microscope. Figure 5.9 represents the transfection efficiency derived from cell counts for each of the three sizes and treatment groups. Figure 5.10 represents the transfection efficiency derived from cell counts for each of the three size treatment groups from lipid outer coating. The same procedure was followed for each of the groups. Our idealized nanoparticles even at bigger size would be one, which can be endocytosed but not just penetrate. The results for the transfection concluded that lipid particles showed higher transfection rate as much as 22% for 126 nm size group. The transfection increased as the volume is increased but for the 210 nm and 1500 nm nanoparticle size group the transfection rate decreased tremendously to nearly 2%. Whereas for the GALA coated nanoparticles even for the size range 126 nm the transfection rate was low as compared to lipid-coated nanoparticle to about 10%. Further increasing the size group at 210 nm the transfection rate remains constant to 10 %. For higher size nanoparticle it is a known fact that there is increase in apoptotic nuclei, which is supported by our results. The difference in the results for GALA and lipid nanoparticles indicates that at even higher size for GALA the particles are endocytosed due to interaction with asialoglycoprotein receptor but not for lipid nanoparticles which might be just penetrating.

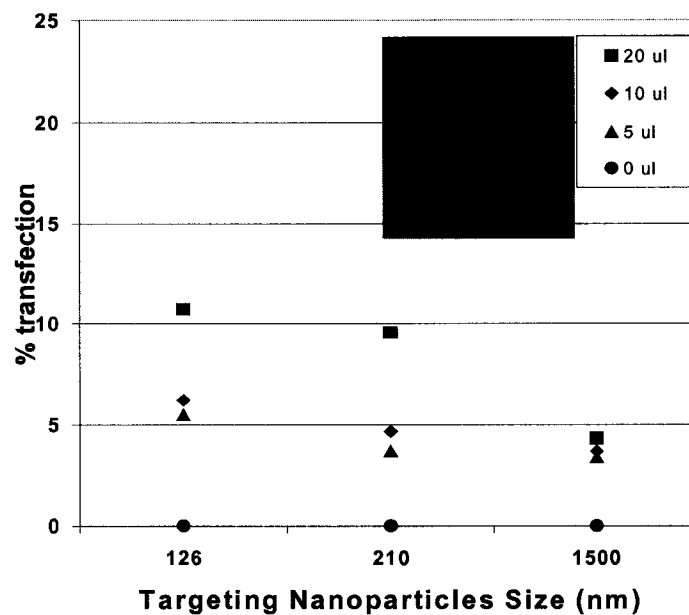


Figure 5.9: Effect of Size on GALA Coated

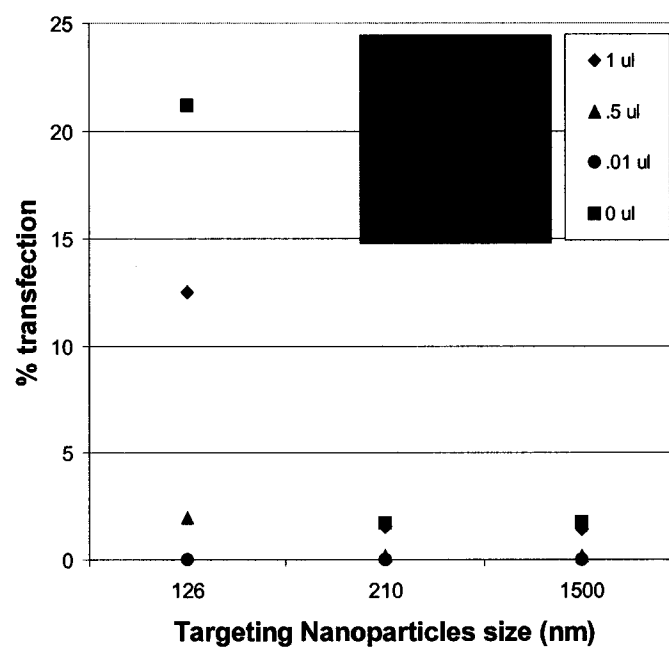


Figure 5.10: Effect of Size on Lipid Coated, Nanoparticle

From the table 5.1 it can be seen that various other architectural nanoparticles were constructed. In the table the construction of different particles is shown and different conditions of their fabrication used Nanoparticle of size 621nm with outer coating as Polygalactosamine, Nanoparticle of size 415nm with outer coating as Polyethyleneimine, Nanoparticle of size 340nm with outer coating as Polyarginine and Nanoparticle of size 185nm with outer coating as Protamine were prepared for DNA delivery. These particles were constructed as it had been reported earlier that these molecules have been used for similar DNA delivery research. It was seen that the uptake of particles was almost 0 % while protamine, polygala, PEI and other targeting moieties were used.. These facts determine that even particles with size less than 200 nanometer were constructed for DNA delivery with outer coating of Protamine but failed to show any transfections rate which was seen earlier for galactosamine coated nanoparticles. Thus layer-by-layer renders the ability to choose specific cell type with receptor binding affinity and target individually with specific outer targeting strategy.

This research has following challenges to overcome:

- Cells are widely known to only allow particles within a particular size range upto 300 nm, to pass the outer membrane. The nuclear membrane is even more tightly guarded, only allowing specific molecules to pass into the nuclear compartment. Passing through these barriers is paramount for the success of DNA delivery. The size of the particles delivered is therefore critical for the success of nanoparticle mediated gene delivery. The major size determinant for

the nanoparticles is the nature of the core particle, onto which the coats are layered as well as the coating materials used.

- The DNA used for this study was of approximate length 2526nm and the silica cores used were of the size range 78nm, hence the particles size distribution, which was characterized, with the help of AFM and Zeta Potential indicated very unclear pattern of fabricated nanoparticles. DNA being so long molecule would eventually have more than 1 core particles around it due to the charge potential, as the silica were coated with positively charged PEI. If the DNA length would be reduced and thereby containing the same gene code for protein expression in the targeted cell type, possibility of constructing such ideals nanoparticles would be evident.

This work was a part of NASA project “Nanoparticles for DNA delivery”.

Table 5.1: Different customized nanoparticles architecture

Sample	Core	Monolayer 1	Monolayer 2	Monolayer 3	Monolayer 4	Monolayer 5	Monolayer 6	Conditions
	Si	PEI	DNA	PEI	DNA			DI Water
	Si	PEI	DNA	PEI	DNA	PEI	BSA	DI Water
505	Si	PEI	DNA	PEI				DI Water
S1	Si	PEI	DNA	PEI	DNA			DI Water
S2	Si	PEI	DNA	PEI	DNA	PEI	Gala	DI Water
S3	Si	PEI	DNA	PEI	DNA			Tris
S4	Si	PEI	DNA	PEI	DNA			Tris + salt
S5	Si	PEI	DNA	PEI	DNA	Gala		Tris
S6	Si	PEI	DNA	PEI	DNA	Gala		Tris + salt
T1	Si	PEI	DNA					DI Water
T2	Si	PEI	DNA	Gala				DI Water
PAH	Si	PAH	DNA					DI Water
PAH1	Si	PAH	DNA	Gala				DI Water
PTREZ	Si	PEI	PBS3 + PTREZ	PEI	PolyGala			DI Water
PTREZ 1	Si	PEI	PBS3 + PTREZ					DI Water
PTREZ 2	Si	PEI	PBS3 + PTREZ	PEI				DI Water
PBI1	Si	PEI	PBS3 + PBI					DI Water
PBI2	Si	PEI	PBS3 + PBI	PEI				DI Water
PBI	Si	PEI	PBS3 + PBI	PEI	PolyGala			DI Water
ARG	Si	PEI(2000)	DNA	PolyArginine				DI Water
PRO	Si	PEI(2000)	DNA	Protamine				DI Water
@	MF	Polygala						DI Water
CT	Si	PEI(2000)	DNA	PolyGala				DI Water
HP	Si	PEI(2000)	DNA	PolyGala				DI Water
Gold 60nm	gold	PEI(2000)	DNA	PolyArginine				DI Water

CHAPTER 6

NANOASSEMBLY OF BIODEGRADABLE MICROCAPSULES FOR DNA ENCASING

6.1 Introduction

In a previous chapter, we described formation of vector (DNA Delivery System) based on nanoparticle construction. In this chapter we have encapsulated DNA in a micro container with biodegradable coating for DNA delivery. The development of layer-by-layer (LbL) self-assembly technology [3, 47, 108, 109] promises a solution to many problems of modern biotechnology. Encapsulation of DNA molecules in micro- and nanovolume is an important goal. Although considerable progress was made in gene therapy and DNA vaccine technology, a problem of DNA degradation upon delivery still remains.[110, 111] It is important to develop a carrier system that can penetrate cell shell and protect plasmid DNA from degradation. Depot and delivery systems such as polymer microparticles prepared using emulsion method, solvent-diffusion nanospheres, and liposome provided an essential progress in DNA delivery. [112-114] However, not

high enough efficiency of encapsulation and needs to engineer the structure and properties of protective shell on nanometer scale provide an avenue for further efforts in this direction. In this work we propose a new “vehicle” for DNA delivery based on microcapsules with 40 nm thick molecularly organized biocompatible shell.

Polyelectrolyte capsules, first reported in [74], are based on application of LbL assembly of nanometer thick polymeric films with controlled composition and properties onto the surface of decomposable tiny cores. A variety of materials (synthetic and natural polyelectrolytes, proteins, multivalent ions, inorganic and organic nanoparticles, lipids) were used as components of the capsule shell providing versatile properties. [68, 74, 115, 116] Macromolecules can be introduced inside the capsules by two ways: first, using encapsulated material as template core, and second, loading macromolecules into preformed polyelectrolyte shell. Adjusting shell permeability by changing a solvent (water-alcohol-acetone), ionic strength or pH allows controlling release of encapsulated compound. [79, 80]

6.2 Microencapsulating DNA and Characterizing

In this study, a novel process of microencapsulating DNA in biocompatible poly[β -glucuronic acid-(1 \rightarrow 3)-N-acetyl- β -galactosamine-6-sulfate-(1 \rightarrow 4)] (known as chondroitin sulfate, Sigma) (PG) / poly(-L-arginine) (PA) capsules of 4 μ m diameter was developed. DNA molecules were deposited by controlled precipitation of DNA/Sperimidine (Sp) complex onto a surface of template microparticles followed by LbL assembly of PA and PG protective biocompatible shell. Large 4 μ m capsules were taken as model to develop DNA encapsulation procedure and understand DNA behavior in capsule volume.

MnCO₃ particles of 4 μm diameter (from PlasmaChem GmbH) were taken as template cores. 0.5 mg/mL MnCO₃ particle suspension (30 ml) was mixed with 1 mL of 1.5 mg/mL DNA solution (highly-polymerized DNA sodium salt from Calf Thymus, Sigma). Precipitation of DNA/Sp complex on template particles was made adding dropwise 2 mL of 1 mg/mL spermidine solution into stirred MnCO₃/DNA solution (Fig. 6.1a,b). Further alternated LbL assembly of biocompatible PA/PG shell was carried out with 1 mg/mL PA or PG solutions (Fig. 6.1b,c). After each deposition step, microparticles were washed out 3 times. A layer-by-layer assembly of polyelectrolyte layers was monitored by electrophoretic mobility measurements (ZetaPlus Zeta Potential Analyzer, Brookhaven Instr. Corp). For each sample, 4 PA/PG bilayers were deposited with PA as the last monolayer and surface potential of the capsule regularly changes from +40 mV for PA to -35 mV for PG, indicating formation of the planned wall composition. 5 nm assembly step for PA/PG was found from parallel PA/PG assembly on QCM electrode (Quartz Crystal Microbalance, USI-System, Japan). Therefore, a total capsule wall thickness was 40 nm. PA capsule outermost was chosen because of its potential to increase translocation activity through the cell membranes.[117, 118] The mass of capsules were measured in another QCM experiment when 8 μL of empty or loaded capsule solution of known concentration was dried on QCM electrode, and their weight was measured.

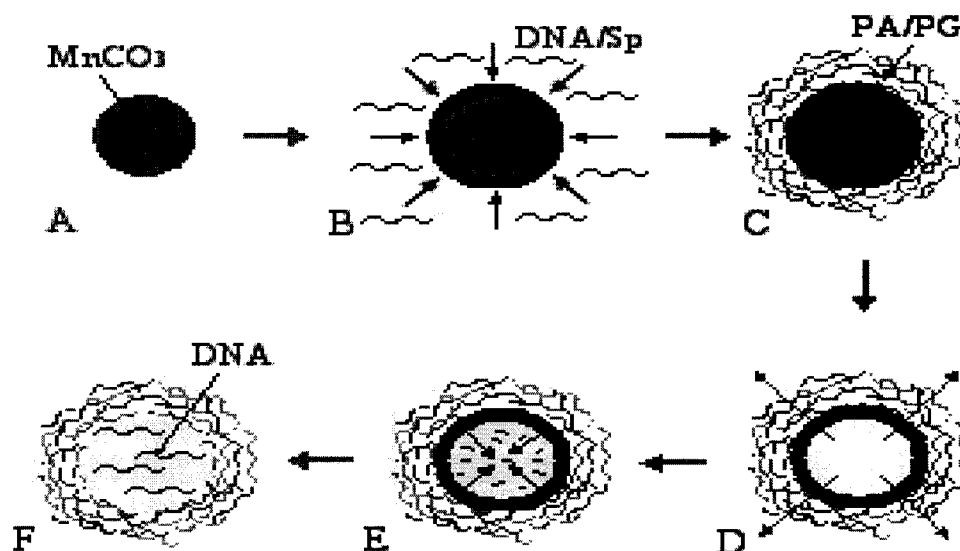


Figure 6.1: Schematic illustration of the DNA encapsulation process. A-B: controlled precipitation of DNA/Sperimidine (Sp) complex on the surface of template particles; B-C: LbL assembly of protective biocompatible shell; C-D: template dissolution; D-E DNA/Sp complex dissolution

At the final step, MnCO_3 template particles were dissolved in deaerated 0.01 M HCl. As a result, biocompatible PA/PG capsules containing DNA/Sp complex were obtained. After removal of the core, the capsules were studied with confocal fluorescence microscopy (Leica DM IRE2 Confocal Fluorescence Microscope). Figure. 6.2a illustrates a typical fluorescence image of (DNA/Sp)PA/PG capsules immediately after dissolution of template. Fluorescence signal is caused by presence of Rhodamine-labeled DNA [115, 119] in the capsule interior. The cross-section profile of fluorescence intensity along the capsule diameter gives the DNA distribution. There are two peaks demonstrating that DNA was confined initially to the inner capsule walls. Then these capsules were treated with 0.1 M HCl for 10 min.

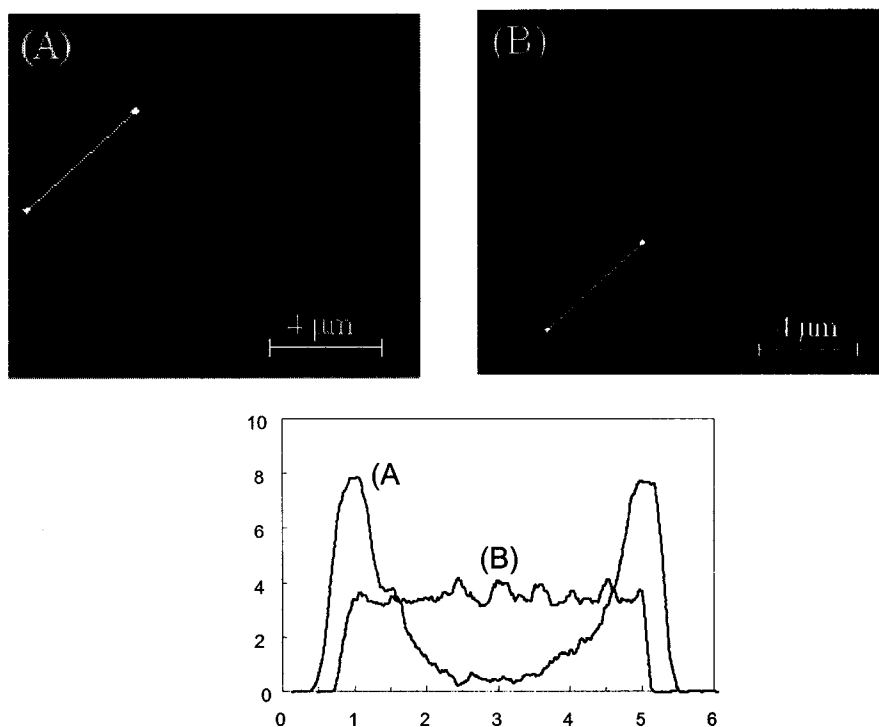


Figure 6.2. Fluorescence confocal microscopy images of the DNA-containing capsules composed of 4 PA/PG bilayers just after decomposition of template core (A) and after dissolution of the inner DNA/Sp complex (B). Areas under the curves are similar. The inset demonstrates the fluorescence profile for both cases

Such treatment leads to the decomposition of DNA/Sp complex formed in aqueous solution at neutral pH. [116] Thus, low-molecular weight sperimidine was released and removed from the capsule interior. Now, the capsule is filled with freely floating DNA molecules, a result proved by fluorescence signal from the whole capsule volume (Fig. 6.2b). The fluorescent signal is distributed evenly over the capsule interior.

During optimization of DNA adsorption we found that 100 % of DNA could be deposited on the template surface from the water solution as DNA/Sp complex. Judging upon precipitation yield, quantity of the capsules in solution ($\sim 10^8$), and mass of DNA captured in one capsule (12 pg as measured using Quartz Crystal

Microbalance), one can estimate the average concentration of DNA in the capsule volume. The average concentration of DNA that is to be encapsulated through L-b-L

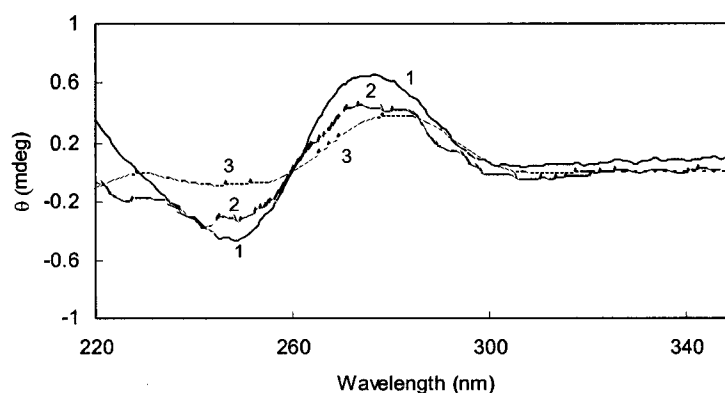


Figure 6.3. Circular dichroism spectra of initial DNA (1); DNA captured in capsule volume (2); DNA in 0.1 M HCl (3).

via DNA/Sp complex 0.4 mg per 1 ml of capsule volume. Due to the helical structure of double-stranded DNA, its circular dichroism (CD) spectrum has a strong signal in 230-350 nm range. [120-122] In Figure 6.3 the CD-spectra of initial DNA, DNA treated with 0.1 M HCl, and DNA captured in capsule volume are compared (Jasco J-810 spectropolarimeter). The spectrum of initial DNA in water solution is typical of the double helix B-conformation of DNA. Adding HCl to DNA solution results in disappearing of negative band at 230-260 nm caused by denaturation of double stranded DNA. [120-122] However, after decomposition of DNA/Sp complex CD spectrum of DNA captured inside PA/PG microcapsules reveals minor changes as compared to initial DNA. Such insignificant changes in diachronic bands for DNA captured inside in all likelihood evidence primary preservation of double helix structure. Apparently, sperimidine and polyarginine partially compensate in capsule volume negative effect of low pH forming pH gradient across the capsule shell which

was previously observed for polyelectrolyte capsules containing polyamines inside.

[123-125]

6.3 Conclusion

In conclusion, we developed a versatile approach for DNA encapsulation inside protective biocompatible polyelectrolyte microshell retaining natural double-helix structure of DNA molecules captured inside. Currently, this technique is employed for targeted delivery of plasmid DNA in living cell using capsules of a smaller diameter (300 nm). We have demonstrated the capability to encase DNA in microcontainers thereby retaining its activity. As following from the previous chapter for better gene delivery one has to make these capsules/nanoparticles smaller in size and it will be the next big challenge.

CHAPTER 7

CONCLUSION

7.1 Enzyme Encapsulation

Thin wall microcapsules were formed via a layer-by-layer self-assembly by eight to ten steps of alternate adsorption of oppositely charged poly(styrenesulfonate) and poly(allylamine) on microcores. After the core dissolution, empty polymeric shells with 20-25 nm thick walls were obtained. These microcapsules were loaded with myoglobin, hemoglobin and glucose oxidase by opening capsule pores at low pH and closing them at higher pH. At the concentration of the loading proteins of 1 mg/mL, they result in ca 30 mg/mL protein concentration. The native structure of the enzyme was not affected due to different treatments and this will open new ways for the use of the microcontainers as reactors, for Bio assay, sensoric devices and other complex application.

7.2 Nanoparticles DNA Delivery Systems

DNA, used as one of the layers in the nanoparticle architecture, was delivered to the cell indicated by the fluorescence. The size parameter was studied for the targeting of the cell type and gene delivery systems. It was shown that for successful transcription the nanoparticle should be less than 300 nm in size and such particles can be easily

endocytosed by cells. This research will enhance the use of DNA as one of the layers in constructing nanoparticles and new designed outer coatings can be further used to target a specific cell type.

7.3 Microencapsulation of DNA as New Gene Vector

In presented work we have made an attempt to elaborate detailed procedure for DNA encapsulation inside biocompatible poly(-L-arginine)/poly(galactosamine) polyelectrolyte capsules of 4 micro meter diameter. This procedure can be further employed for preparation of nanosized DNA-containing polyelectrolyte microcontainers for target DNA delivery in cell. It was shown that the encapsulated DNA preserves its initial native structure. This system would be a model systems and a challenge for fabricating DNA delivery vector that can be easily endocytosed and thereby curing many diseases.

REFERENCES

- 1 A. Ulman, Academic Press, Boston, pp.1-440, 1991
- 2 R. Iler, *J. Colloid Interf. Sci.* 21, 569 (1966)
- 3 G. Decher, *Science* 227, 1232 (1997)
- 4 S. Keller, H.-N. Kim, and T. Mallouk, *J. Am. Chem. Soc.* 116, 8817 (1994)
- 5 G. Decher and J.-D. Hong, *Ber. Bunsenges. Phys. Chem.* 95, 1430 (1991)
- 6 Y. Lvov, G. Decher, and H. Möhwald, *Langmuir* 9, 481 (1993)
- 7 Y. Lvov, G. Decher, and G. Sukhorukov, *Macromolecules* 26, 5396 (1993)
- 8 Y. Lvov, F. Eessler, and G. Decher, *J. Phys. Chem.* 97, 13773 (1993)
- 9 Y. Lvov, H. Haas, G. Decher, H. Möhwald, and A. Kalachev, *J. Phys. Chem.* 97, 12835 (1993)
- 10 G. Decher, F. Essler, J.-D. Hong, K. Lowack, J. Schmitt, and Y. Lvov, *polym. Prep.* 34, 745 (1993)
- 11 G. Decher, Lvov, and J. Schmitt, *Thin Solid Films* 244, 772 (1994).
- 12 Y. Lvov, H. Hass, G. Decher, H. Möhwald, A. Mikhailov, B. Mtchedlishvily, E. Morgunova, and B. Vainshtein, *Langmuir* 10, 4232 (1994)
- 13 Y. Lvov and G. Decher, *Crystallogr. Rep.* 39, 628 (1994)
- 14 G. Decher, M. Eckle, J. Schmitt, and B. Struth, *Curr. Opin. Colloid Interf. Sci.* 3, 32 (1998)
- 15 Y. Lvov, K. Ariga, and T. Kunitake, *Colloid Surf. A* 146, 337 (1999).
- 16 D. Yoo, J. Lee, and M. Rubner, *Mater. Res. Soc. Symp. Proc.* 413, 395 (1996)

- 17 T. Cooper, A. Campbell, and R. Crane, *Langmuir* 11,2713 (1995).
- 18 K. Ariga, Y. Lvov, and T. Kunitake, *J. Am. Chem. Soc.* 119, 2224 (1997).
- 19 Y. Lvov, S. Yamada, and T. Kunitake, *Thin Solid Films* 300, 107 (1997).
- 20 E. Kleinfeld and G. Ferguson, *Science* 265, 370 (1994).
- 21 Y. Lvov, K. Ariga, I. Ichinose, and T. Kunitake, *Langmuir* 13, 6195 (1997).
- 22 Y. Lvov, B. Munge, I. Ichinose, S. Suib, and J. Rusling, *Langmuir* 16, 8376 (2000).
- 23 Y. Lvov, K. Ariga, and T. Kunitake, *Langmuir* 12, 3038 (1996).
- 24 T. Cassageneau, J. Fenlder, and T. Mallouk, *Langmuir* 16, 241 (2000).
- 25 F. Caruso, A. Sussha, M. Giersig, and H. Möhwald, *Adv. Mater.*, 11, 950 (1999).
- 26 K. Ariga, Y. Lvov, M. Onda, I. Ichinose, and T. Kunitake, *J. Appl. Clay Sci.* 15 137 (1999).
- 27 S. Joly, R. Kane, L. Radzilovski, T. Wang, A. Wu, R. Cohen, E. Thomas, and M. Rubner, *Langmuir* 16, 1354 (2000).
- 28 Y. Lvov, K. Ariga, and T. Kunitake, *Chem. Lett.* 2323 (1994).
- 29 Y. Lvov, K. Ariga, I. Ichinose, and T. Kunitake, *J. Am. Chem. Soc.* 117, 6117 (1995).
- 30 Y. Lvov, in "Protein Architecture: Interface Molecular Assembly and Immobilization Biotechnology" (Y. Lvov and H. Möhwald, Eds.), Ch. 6, Marcel Dekker, New York, 2000
- 31 Y. Lvov, K. Ariga, I. Ichinose, and T. Kunitake, *J. Chem. Soc. Chem. Commun.* 2313 (1995).
- 32 M. Onda, Y. Lvov, K. Ariga, and T. Kunitake, *J. Ferment. Bioeng.* 82, 502 (1996).
- 33 M. Sano, Y. Lvov and T. Kunitake, *Ann. Rev. Material Science* 26: 153 (1996).
- 34 N. Hoogeveen, M. Cohen Stuart and G. Fler, *Langmuir* 12: 3675 (1996).
- 35 Y. Lvov, J. Rusling, D. Thomsen, F. Papadimitrakopoulos, T. Kawakami and T. Kunitake, *Chem. Commun.*, 1229 (1998).
- 36 Frank Caruso, Rachel A. Caruso, Marina Spasova, Andrei Sussha, Michael Giersig,; *Chem. Mater.* 2001, 13, 109-116

- 37 David Gittins and Frank Caruso, ; J. Phys. Chem. B2001, 105, 6846-6852
- 38 Tomonori Hoshi, Hidekazu Saiki, Sachie Kuwazawa, Chikako Tsuchiya,; Anal Chem. 2001, 73, 5310-5315
- 39 Sukhorukov, G.B; Frank Caruso, Helmuth Mohwald,; Polymers for Advanced Technologies, 9 759-767, 1998
- 40 Gao. M.Y.; Richter, B.; Kirstein. S.; Mohwald, J. Phys. Chem B1998, 102, 4096-4103
- 41 Ferreira, M.; Cheung, J.H.; Rubner, M.F. Thin Solid Films 1994, 244, 806-809
- 42 Cheung, J.H.; Fou, Rubner, M.F. Thin Solid Films 1994, 244, 985-989
- 43 Katz, H.E.; Scheller, G.; Putvinski, T.M.; Schilling, M.I.; Wilson, W.L.; Chidsey, C.E.D. Science 1991, 254, 1485
- 44 Keller, S.W.; Johnson, S.A.; Yonemoto, E.H.; Brigham, E.S.Mallouk, T.E. J. Am. Chem. Soc. 1995, 117, 12879-12880
- 45 D. Elbert, C. Herbert, and J. Hubbell, Langmuir 15, 5335 (1999).
- 46 V. Tsukruk, F. Rinderspacher, and V. Bliznyuk, Langmuir 13, 2171 (1997).
- 47 Y. Lvov and G. Decher, Crystallography Reports 39: 628 (1994)
- 48 N. Hoogeveen, M. Cohen Stuart and G. Fleer, Langmuir 12: 3675 (1996).
- 49 M. Onda, Y. Lvov, K. Ariga and T. Kunitake, Biotechnology and Bioengin. 51: 163 (1996).
- 50 J. Park, B. Muhoberac, P. Dubin and J. Xia, Macromolecules 25: 290 (1992).
- 51 M. Roberts, G. Lindsay, W. Herman and K. Wynne, J. Am. Chem. Soc. 120: in press (1998).
- 52 K. Ariga, M. Onda, Y. Lvov and T. Kunitake, Chemistry Lett., 25 (1997).
- 53 E. Brynda and M. Houska, J. Colloid and Interface Sci. 183: 18 (1996).
- 54 Y. Sun, X. Zhang, C. Sun, B. Wang and J. Shen, Macromol. Chem. Phys. 197: 147 (1996).
- 55 S. Brock, M. Sanabria, S. Suib, V. Urban, P. Thiyagarajan and D. Potter, J. Am. Chem. Soc. 120: in press (1998).

- 56 Zhang, Y. Sun, and J. Shen, in "Protein Architecture: Interfacial Molecular Assembly and immobilization Biotechnology" (Y. Lvov and H. Möhwald, Eds.), Marcel Dekker, New York, 2000.
- 57 F. Caruso, N. Furlong, K. Ariga, I. Ichinose and T. Kunitake, *Langmuir* 14 , 4559 (1998).
- 58 Y. Lvov, Z. Lu, X. Zu, J. Schenkman, and J. Rusling, *J. Am. Chem. Soc.* 120, 4073 (1998).
- 59 M.E. Bobreshova, Sukhorukov, G.B.; E.A. Saburova, L.I. Elfimova, B.I. Sukhorukov and L.I. Sharebehina, *Biophysics*, 44 (1999) 813-820.
- 60 A. Antipov, Sukhorukov, G.B.; E. Donath, Mohwald, H., *J. Phys. Chem. B*, 105, 2001, 2281-2284
- 61 Donath, E.; Sukhorukov, G.B.; Caruso, F.; Davies, S.F.; Mohwald, H. *Angew. Chem. Int. Ed.* 1998,37,2202-2205
- 62 Sukhorukov, G.B.; Donath, E.; Lichtenfeld, H.; Knippel, E.; Knippel, M.; Buddle, A. Mohwald, H. *Colloids surfaces A: Physicochem. Eng. Aspects* 1998, 137, 253.
- 63 Caruso, F.; Yang, W.; Tran, D.; Renneberg, R. *Langmuir* 2000, 16, 8932
- 64 Arys, X.; Jonas, A.M.; Laschewsky, A.; Legras, R. In *Supramolecular Polymers*; Ciferri A., Ed.; Marcel Decker: New York, 2000; p. 505.
- 65 Bertrand, P.; Jones, A.; Laschevsky, A.; Legras, R. *Macromol. Rapid Commun.* 2000, 21, 319.
- 66 Sukhorukov, G.B.; E. Donath, S. Moya, A.S Susha, A Voigt, J. Hartmann and Mohwald, H., *J. Microencapsulation*, 17(2000) 177-185
- 67 G. Sukhorukov, Mohwald, H., Edwin Donath; ; *J Phys. Chem. B*1999, 103, 6434-6440
- 68 D. Mobius and R. Miller, *Novel Methods to Study Interfacial Layers*; Vol 11 Studies in Interface Science
- 69 Y. Lvov, A.A. Antipov, Sukhorukov, G.B.; E. Donath, Mohwald, H., *Macromol. Rapid Commun.* 2001, 22, 44-46
- 70 J.D. Mendelsohn, C.J. Barrett, V.V. Chan, A.J. Pal, A.M. Mayes and M.F. Rubner, *Langmuir*, 16(2000) 5017-5023

- 71 Regine V. Klitzing, and Mohwald, H., *Macromolecules*, 1996, 29, 6901-6906
- 72 Y. Lvov, A.A. Antipov, Sukhorukov, G.B.; E. Donath, Mohwald, H., *Nanoletters*; 02/26-2001,
- 73 Sukhorukov, G.B.; E. Donath, Möhwald, H., Lars Dahne, Jurgen Harumann; *Advanced Materials*; 2000, 12. No 2
- 74 Sukhorukov, G.; Donath, E.; Davis, S.; Lichtenfeld, H.; Caruso, F.; Popov, V.; Möhwald, H. *Polymers Advanced Techn.* 1998, 9, 759-767.
- 75 Caruso, F.; Trau, D.; Möhwald, H.; Renneberg, R. *Langmuir* 2000, 16, 1485.
- 76 Moya, S.; Donath, E.; Sukhorukov, G.; Auch, M.; Bäumer, H.; Lichtenfeld, H.; Möhwald, H. *Macromolecules* 2000, 33, 4538.
- 77 Sukhorukov, G.; Antipov, A.; Voigt, A.; Donath, E.; Möhwald, H. *Macromol. Rapid Comm.* 2001, 22, 44.
- 78 Antipov, A.; Sukhorukov, G.; Leporatti, S.; Radchenko, I.; Donath, E.; Moehwald, H. *Colloids and Surfaces A* 2002, 198, 535.
- 79 Tiourina, O.; Antipov, A.; Sukhorukov, G.; Lvov, Y.; Möhwald, H. *Macromol. Bioscience* 2001, 1, 209.
- 80 Lvov, Y.; Antipov, A.; Mamedov, A.; Möhwald, H.; Sukhorukov, G. *Nano Letters* 2001, 1, 125.
- 81 Gao, C.; Liu, X.; Shen, J.; Möhwald, H. *Chem. Comm.* 2002, 1928.
- 82 Ai, H.; Jones, S.; De Villiers, M.; Lvov, Y. *J. Controlled Release* 2003, 86, 54.
- 83 Shenoy, D.; Antipov, A.; Sukhorukov, G.; Möhwald, H. *Biomacromolecules* 2003, 4, 265.
- 84 Loury, O.; Rosenbrough, N.; Farr, A.; Randall, R. *J. Biol. Chem.* 1951, 193, 265.
- 85 Onda, M.; Ariga, K.; Kunitake, T. *J. Bioscience Bioengin.* 1999, 87, 69.
- 86 Huang, Q.; Lu, Z.; Rusling, J. *Langmuir* 1996, 12, 5472.
- 87 Kabanov, V. *Polymer Science* 1996, 36, 143.
- 88 Gao, C.; Leporatti, S.; Donath, E.; Möhwald, H. *J. Phys. Chem. B* 2000, 104, 7144.
- 89 Sellergren, B., Swietlov, A., Ambert, T., Unger, K. *Anal. Chem.* 1996, 68, 402

- 90 Zhang, X, Gao M, Kong X, Sun Y, Shen J, J. Chem. Soc., Chem Commun, 1994, 1055
- 91 Ichinose I., Fujiyoshi K., Mizuki, S, Lvov Y., Kunitake, T., Chem Lett. 1996, 257
- 92 T Cassagneau, T Mallouk, J. Fendler, J. Am. Chem. Soc. 120 (1998) 7848
- 93 Y. Lvov, Price R, Colloids And Surfaces B: Biointerfaces 23 (2002) 251-256
- 94 Langer, R. Nature, 1998, 392, 5-10
- 95 Hari, P. R., Chandy, T., Sharma, C. P. J Microencapsulation 1996, 13, 319
- 96 Kreuter, J Colloidal Drug Delivery Systems, Marcel Dekker: New York, 1994
- 97 Mahato, R I., Smith, L. C., Rolland, A. (1999) Pharmaceutical perspectives of nonviral gene therapy, Adv Genet. 41: 95-156
- 98 Gilding, D.K. Biocompatibility of Clinical Implant Materials, Vol. 2; CRC Press: Boca Raton, 1981
- 99 Shea, L.D.; Smiley, E.; Bonadio, J.; Mooney, D. J. DNA delivery from polymer matrixes for tissue engineering. Nature Biotechnol. 1999, 17,551-4
- 100 Sang-oh Han, Ram Mahota, Sung Wan Kim, Molecular Therapy, 2, 2000, 302-317
- 101 VS Trubetskoy, SC Wong, VG Budker, A Loomis, JE Hagstrom, JA Wolff, Gene Therapy, 10, 2003,261-271
- 102 Vladmir Trubetskoy, Aaron Loomis, James Hagstrom, Vladmir Budker, Jon Wolff, Nucleic Research, 27, 1999, 3090-3095
- 103 Ji Zheng, William S Manuel, Peter J. Hornsby, Biotechnol. Prog. 2000, 16, 254-257
- 104 Karine Fabio, Jerome Gaucheron, Christophe Di Giorgio, Pierre Vierling, Bioconjugate Chem, 2003, 14, 358-367
- 105 Shiroh Futak, Tomaki Suzuki, Wakana Ohashi, Takeshi Yagame, Yukio Sugiura, The Journal of Biological Chemistry, vol 276, 8, 5836-5840, 2001
- 106 MA Arangoa, N Duzgunes, C Tros de Ilarduya, Gene Therapy, 10, 2003, 5-14
- 107 Jeanette T. Tsai, Kevin J. Furstoss, Timothy Michnick, David L. Sloane, Ralph W. Paul, Biotechnol. Appl. Biochem, 36, 2002,13-20

- 108 Schlenoff, J. B.; Dubas, S.T. *Macromolecules* 2001, *34*, 139-160
- 109 Harris, J.J.; Stair, J.L.; Bruening, M.L. *Chem. Mater.* 2000, *12*, 1941-1946.
- 110 Jong, Y.S.; Jacob, J.S.; Yip, K.P.; Graham, G.; Ellen, S.; Marsha, W. *J. Control. Release* 1997, *47*, 123-134.
- 111 Pachuk, C.J.; McCallus, D.E.; Weiner, D.B.; Satishchandran, C.; *Curr. Opin. Mol. Ther.* 2000, *2*, 188-198.
- 112 Zhuang, F. F.; Liang, R.; Zou, C. T.; Ma, H.; Zheng, C. X.; Duan, M. X. *J. Biochem. Biophys. Methods* 2002, *52*, 169-178.
- 113 Bailey, A. L.; Sullivan, S. M. *Biochim. Biophys. Acta* 2000, *1468*, 239-252.
- 114 Hirose, S.; Muller, B. G.; Mulligan, R. C.; Langer, R. *J. Control. Release* 2001, *70*, 231-242.
- 115 Ibarz, G.; Dahne, L.; Donath, E.; Möhwald, H. *Adv. Mater.* 2001, *13*, 1324-1327.
- 116 Schüler, C.; Caruso, F. *Biomacromolecules* 2001, *2*, 921.
- 117 Futaki, S.; Suzuki, T.; Wakana, O.; Yagami, T.; Tanaka, S.; Ueda, K.; Sugiura, Y. *J. Biol. Chem.* 2001, *276*, 5836-5840.
- 118 Mittal, S.; Aggarwal, N.; Sailaja, G. *Vaccine* 2001, *19*, 253-263.
- 119 Evenson, D.; Darzynkiewicz, Z.; Jost, L.; Janca, F.; Ballachey B. *Cytometry* 1986, *7*, 45-53.
- 120 Del Vecchio, P.; Esposito, D.; Ricchi, L.; Barone, G. *Int. J. Biol. Macromol.* 1999, *24*, 361-369.
- 121 Gray, D.M.; Ratliff, R.L.; Vaughan, M.R. *Methods Enzymol.* 1992, *211*, 389-406.
- 122 Raspaud, E.; Olvera de la Cruz, M.; Livolant, F. *Biophysical journal* 1998, *74*, 381-390.
- 123 Sukhorukov, G.B.; Brumen, M.; Donath, E.; Möhwald, H. *J. Phys. Chem. B* 1999, *103*, 6434-6439.
- 124 Radtchenko, I.L.; Giersig, M.; Sukhorukov, G.B. *Langmuir* 2002, *18*, 8204-8206.
- 125 Shchukin, D.G.; Radtchenko, I.L.; Sukhorukov, G.B. *J. Phys. Chem. B* 2003, *107*, 86-90.

VITA

Report of Invention

- “Long lasting hydrophilic, biocompatible nanocoating with layer-by-layer assembly of titanium dioxide nanoparticles and polyanion” (Disclosure filed)

Given Talk

- University of Texas Medical Branch Galveston, Texas, August 2003
”Sequential Layer-by-Layer Assembly for Biotechnological Applications”

Journal and Conference Publications

- Dmitry Schukin, **Amish Patel**, Gleb Sukhorukov, Yuri Lvov
“*Nanoassembly of Biodegradable Microcapsules for DNA Encasing*,”
JACS (Journal of American Chemical Society), 2004, v.126, 3374-3376
- Nitin Gupta, **Amish Patel**, Yuri Lvov, M. McShane, James Palmer
“*Study of Transport Phenomena of FITC-labeled Dextran through Nano Self-Assembled Micro-shells*,” Colloid Surface A, 245(2004) 137-142
- R. Ghan, T. Shutava, **A. Patel**, V. John, Y. Lvov, “*Enzyme catalyzed polymerization within polyelectrolyte microcapsules*,” Macromolecules, 37 (12), 4519 – 4524, 2004
- Y. Lvov, T. Cui, F. Hua, **A. Patel**, A. Antipov, A. Cordeiro, M. Prevot, G. Sukhorukov, R. Besser, “*Layer-by-layer nanoassembly of polyion and enzymes for production of micropatterns and nanoshells*,” Published in SPIE-Proceedings 2003 (SPIE International Nanotechnology and BioMEMs Conference) 2003, v.5505
- R. Ghan, T. Shutava, **A. Patel**, V. John, Y. Lvov, “*Layer-by-Layer Engineered Microreactors for Bio-Polymerization of 4-(2-aminoethyl) phenol hydrochloride*,” *Mat. Res. Soc. Symp. Proc.*782, pp. A5.43.1 – A5.43.6, 2003
- Nitin Gupta, **Amish Patel**, Michael McShane, James Palmer
“*Study of Transport Phenomenon of FITC labeled Dextran through nanoself assembled microshells*,” Published AICHe 2003 Annual Meeting Conference Proceedings
- Dinesh Kommireddy, **Amish Patel**, Tatsiana Shutava, David Mills, Yuri Lvov
“*Nanoorganized thin films for surface modification and biocompatible coatings*,” Submission pending in November 2004

Conference Presentation with Published Abstracts

- **Amish Patel**, Tarl Prow, Tatsiana Shutava, James Leary, Yuri Lvov
“Layer by Layer fabricated nanoparticles for targeted Gene Delivery,” New York, NY at ACS (American Chemical Society) National Meeting in September 2003.
- Dmitry Schukin, **Amish Patel**, Gleb Sukhorukov, Yuri Lvov
“DNA encapsulation inside biocompatible polyelectrolyte microcapsules,” New York, NY, ACS (American Chemical Society) National Meeting, September 2003.
- **Amish Patel**, Tarl Prow, Tatsiana Shutava, James Leary, Yuri Lvov
“Non-Viral vectors for Gene Therapy,” ACS South west Regional Meeting, Dallas, TX (Sept 29-Oct 2) 2004
- **Amish Patel**, Dinesh Kommireddy, Tatsiana Shutava, Yuri Lvov
“Nanoorganized biocompatible thin films for surface modifications,” ACS South west Regional Meeting, Dallas, TX (Sept 29-Oct 2) 2004
- **Amish Patel**, Tarl Prow, James Leary, Yuri Lvov
“Layer by Layer fabricated nanoparticles for targeted Gene Delivery,” Biomedical Engineering Society Annual Meeting, Nashville TN, October 2003.
- Rohit Ghan, Tanya Shutava, **Amish Patel**, Vijay John, Yuri Lvov
“Layer-by-Layer Engineered Microreactors for Bio-Polymerization of 4-(2-aminoethyl)phenol Hydrochloride,” Boston, MA at Materials Research Society Annual Fall Meeting in December 2003.
- **Amish Patel**, Yuri Lvov, M. McShane, James Palmer
“Loading and Release of Fluorescein Isothiocyanate Labeled Dextran into Nano Self-Assembled Micro- Shells,” NSF, BoR EPSCoR at Baton Rouge, LA in April 2002.
- Nitin Gupta, **Amish Patel**, Yuri Lvov, M. McShane, James Palmer,
“Release study of FITC labeled dextran through microcapsules,” ACS South west Regional Meeting, Austin, TX (Nov 2-4) 2002
- **Amish Patel**, Yuri Lvov, “A novel Approach for Gene Therapy,” New Dreams Symposium 2003, Biomedical Engineering at Louisiana Tech University